LBL--27271

DE89 014894

Vertical Gradient Freeze GaAs: Growth and Electrical Properties

Maria L. Galiano

Center for Advanced Materials
Materials and Chemical Sciences Division
1 Cyclotron Road, Lawrence Berkeley Laboratory
Berkeley, CA 94720

and

Materials Science and Mineral Engineering Department
University of California
Berkeley, CA 94720

May 1989

This work was supported by the Director, Office of Energy Research, Office of Basic Energy Sciences, Materials Sciences Division of the U.S. Department of Energy under Contract No. DE-AC03-76SF00098.

Vertical Gradient Freeze GaAs: Growth and Electrical Properties

by

Maria Lucia Galiano

ABSTRACT

We have investigated the influence of silicon contamination prevention methods on the electrical properties of GaAs grown by the Vertical Gradient Freeze (VGF) technique. We report the effectiveness of these methods for GaAs crystals grown from two different starting materials: n-type with resistivities in the range of 10^{-1} to 10^{3} Ω·cm and semi-insulating (SI) with a resistivity of 10^{8} Ω·cm. We have found that the impurities in the starting materials, specifically boron, carbon and silicon, have an effect on the ability to control silicon contamination with methods that have been reported previously in the literature. We also report the attainment of SI crystals using a PBN crucible, a SI charge and B_2O_3 encapsulation.

ACKNOWLEDGEMENTS

I would like to thank Prof. Eugene Haller for his guidance throughout my two years at Berkeley, especially in regards to my master's thesis. A very special thanks to Dr. Edith Bourret for her supervision and support on my masters project. The hours of informative discussion and her willingness to share her expertise on crystal growth are deeply appreciated. I am grateful to Joe Guitron for teaching me the art of crystal growth and for laughing with me through many a tedious afternoon in the GaAs lab.

I would like to thank Prof. Eicke Weber for reading my thesis, James Heyman for providing the LVM measurements, Dave Nolte for his help with the DLTS measurements and Mark Hoinkis for the EPR measurements.

The love and support of my family from the East Coast has been very helpful. Thanks Mom, Dad, Mel, Ang, Tom, Stef, Gary, Pam and Allison. My friends have been a great resource also. Friday afternoons with the Fools at the Rock helped me keep my sanity. Lynne, my roommate and writing consultant, thanks for the constructive comments on this document and for listening to all of my complaints along the way. Most of all, thanks to Mark for all the hugs and smiles of encouragement from day to day when I needed them the most.

TABLE OF CONTENTS

1. INTRODUCTION

The continually increasing application of semiconductor based electronics creates an enormous demand for high quality semiconducting single crystals. The volume of Si production, for example, is over 3000 metric tons per year[1]. Since the discovery and development of the semiconducting properties of III-V semiconductors by Welker[2] in 1952, these materials have gained importance for the production of electronic devices, e. g., light-emitting diodes (LED's), lasers, microwave devices, etc. The most important binary III-V semiconductors are GaAs, AlAs, GaP, InP, InAs and InSb. One advantage of the III-V's GaAs and InP for optoelectronic applications is that they have a direct band gap. Direct gap semiconductors are orders of magnitude more efficient in emitting light than are the indirect band gap semiconductors, Si and Ge. Both photon emission and absorption can occur without the involvement of lattice phonons.

GaAs and InP have fixed band gaps and lattice constants. Ternary and quaternary compounds, which are usually synthesized from the binary III-V compounds and deposited epitaxially on a binary compound substrate, have band gaps which depend on composition. By controlling the composition, the gap can be tailored for the desired application. Figure 1 is a plot of the energy gap versus lattice constant for the various semiconductors. Solid lines represent direct gap and dashed lines represent indirect gap semiconductors. The figure can be used to select a lattice matched alloy system for a desired application. Lattice mismatch between the substrate and epitaxial layers is undesirable because it creates misfit dislocations and crystalline imperfections in the epitaxial layers which can lead to nonradiative recombination. Examining figure 1, one recognizes that GaAs is lattice matched to AlAs. This has resulted

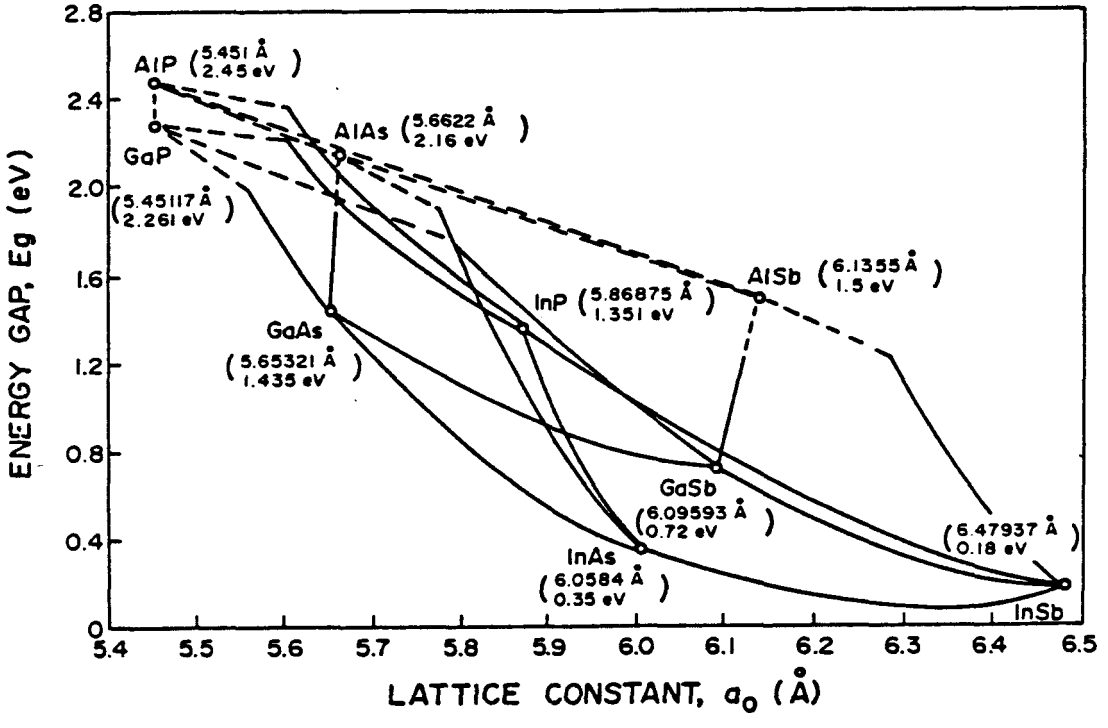

Figure 1. A plot of energy gap versus lattice constant for major III-V semiconductor compounds.

in a large family of high-performance GaAs/AlGaAs devices including photodiodes, solar cells, LED's, injection lasers[3] and more recently high speed transistors[4].

As stated previously, GaAs is the material of choice for use in optoelectronic devices and circuits, since silicon is such a poor light emitter. It was the optoelectronic applications, specifically high powered lasers and light-emitting diodes (LED's), that drove the materials and device development of GaAs for the first two decades[5]. Heavily doped n-type (n^+) GaAs is used for optoelectronic applications. It is usually doped with Si or Te to a free carrier concentration of 10^{18} cm^{-3} and is characterized by a low resistivity (10^{-3} Ω-cm). The two main growth techniques used to produce n^+ GaAs are horizontal Bridgman (HB) and Liquid Encapsulated Czochralski (LEC). Both are capable of producing doped crystals with the necessary quality for optoelectronic applications.

Semi-insulating GaAs has begun and will continue to play an important role in the future in the field of communication and computer technology because of its higher electron mobility and smaller power consumption compared to silicon. The carrier mobility of GaAs is over six times that of Si for 10^{17} cm^{-3} n-type doped substrates. In addition, the peak drift velocity in GaAs is almost twice that in Si and occurs at a much lower electric field. Hence, GaAs devices can operate faster and at lower power than Si devices.

New GaAs device technologies including digital integrated circuits, monolithic microwave integrated circuits (MMICs)[6] and charge coupled devices (CCDs) have adopted ion implantation as a key fabrication technique for the formation of doped layers. The digital circuits have been realized with ion-implanted FETs[7], selectively doped heterostructures (SDHTs)[8], and heterostructure bipolar transistors (HBTs)[9]. This emergence of high-

performance GaAs IC technologies and the stringent demands on wafer quality required by ion implantation have accelerated the demand for high quality, large diameter semi-insulating (SI) substrates. Semi-insulating GaAs crystals have high resistivities (10^8 Ω-cm) and low free carrier concentrations (10^7-10^9 cm^{-3}). These characteristics are desirable because they eliminate unwanted capacitance effects and make SI substrates suitable for fabrication of electrically isolated devices and circuits by direct ion implantation techniques[10].

At present, real medium and large-scale integration of GaAs digital circuits has emerged. Several major computer manufacturers have decided to incorporate GaAs devices in their next generation machines. This choice was based primarily on the speed advantage of these circuits. Monolithic microwave integrated circuits are entirely fabricated with GaAs technology because of the power capabilities of the GaAs FET. In addition, at microwave frequencies, i.e. in the GHz range, GaAs FETs exhibit the lowest noise figure of any three-terminal solid-state device and hence are utilized as front-end amplifiers[6].

GaAs has become a material of "today"[5], with "tomorrow" bringing only more and larger applications to which its technology will be applied. Yet it is not a technology that will replace Si VLSI. Rather, it is an "opportunity technology" which will be applied to those new efforts that are not fully compatible with Si technology[5]. An example of the silicon technology which cannot be realized with GaAs is the silicon MOS technology. Si MOS technology capitalizes on the fact that SiO_2, a very stable insulator with an extremely low surface state density, can be easily grown on the silicon surface. Insulators are necessary for the production of MIS devices. So far, no insulator has been found for GaAs which generates a sufficiently low interface state density for successful MIS device operation.

InP has recently become important because it is a material which can be used as a substrate for the epitaxial production of electro-optical devices for the fiber optical communication systems working in the 1.3 to 1.55 μm wavelength region. The ability to tailor the properties of the quaternary alloy, GaInAsP, grown on InP, has resulted in promising lightwave applications in the long wavelength region.

The technologies for the growth of GaAs and InP crystals is less developed than for Si. However, these technologies are constantly improving, as can be seen by the literature review to follow. The technique for GaAs growth of substrate material for IC fabrication must be able to produce material that has the following characteristics: (1) large, uniform, circular wafers; (2) reproducible and high resistivity; (3) low background impurity levels; and (4) high degrees of crystalline perfection[10]. Most SI GaAs single crystals are currently produced by LEC, a technique capable of meeting, at least in part, the above requirements. The new technique explored in this study should be able to better meet requirements 1, 2 and 4. Results published in the last several years have shown strong indications that it will produce material of higher quality than the material produced by LEC.

1.1 Semi-insulating GaAs

The key to the reproducible growth of undoped semi-insulating GaAs is control over melt-stoichiometry and impurity content. Holmes[11] has shown that melt stoichiometry controls the compensation in undoped LEC GaAs. It is also known that SI behavior is very dependent on native defects such as the deep donor, EL2[11]. The residual impurities present in the material cause deep as well as shallow levels in the crystal. Examples of these shallow donor and acceptor impurities in GaAs are Si and C, respectively. The free carrier

concentration, n, depends on the balance between the deep and shallow donors and acceptors. A proper balance is required for compensation so that SI material is attained. In a simplified three level compensation model[12,13], shown in figure 2, the following two criteria must be met in order to obtain SI material: the number of shallow acceptors, N_A, must be greater than the number of shallow donors, N_D, and the number of deep donors, N_{DD}, must be greater than (N_A-N_D).

1.2 Crystal Growth

Bulk GaAs crystal growth is a process that has been worked on for many years. As mentioned above, at present there are two techniques used to accomplish this solidification process: LEC and HB. Czochralski[14] first published his technique for crystal growth in 1917. The basic concept of the technique as it is used today is this: a single crystal seed is lowered into a melt of the desired material and the temperature of the melt is reduced until crystalline material begins to solidify on the seed; the seed is then raised at a uniform rate and a crystal is pulled from the melt. By changing the power input to the furnace, the temperature of the melt can be changed. This adjusts the axial and radial temperature gradients which in turn affect the crystal diameter. Due to the thermal asymmetries of the furnace, the crystal must be rotated to maintain its cylindrical shape. Stirring of the melt is usually achieved by counter-rotation of the seed and crucible. Advantages of this technique include: the visualization of the growth process, which permits the ability to control the seeding; the relatively high growth rate due to the steep axial temperature gradient; and the ease of doping, if desired.

A problem with this design is that volatile materials or materials with volatile components cannot be pulled by the simple Czochralski technique (CZ).

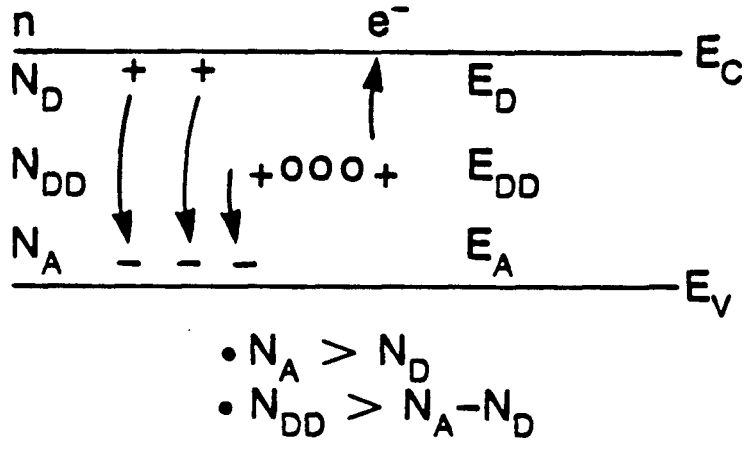

XBL 8711-5987

Figure 2. The three level compensation model. Criteria for SI material: $N_A > N_D$ and $N_{DD} > (N_A - N_D)$.

Crystal growth from a stoichiometric melt without loss of a volatile component can be achieved if the entire surface of the containing vessel is kept at an elevated temperature at which the vapor pressure of the volatile element is equal to or large than the dissociation pressure over the melt. These temperatures become quite substantial for arsenide or phosphide compounds (550 - 700°C) and cannot be maintained in standard CZ pullers. Special, more sophisticated high pressure pullers had to be developed. Gremmelmaier[15] developed an all hot puller with a magnetic lifting mechanism to control the movement of a seed crystal in a sealed system.

Metz et. al.[16] developed the liquid encapsulation (LE) technique whereby the exposed surface of the melt is covered by a confining liquid. They reported good quality single crystals of PbTe grown with a B_2O_3 encapsulant. B_2O_3 is a rather viscous molten glass above its softening point, 450°C. Its viscosity is too great to permit its use below 800°C. It tends to cling to the pulled crystal, covering a large fraction of the surface, preventing the volatile material from leaving the surface as the crystal cools. B_2O_3 is transparent, which allows for direct observation of the solid-melt interface and it is soluble in hot water, so it is easily removed. B_2O_3 is also useful in that it is thermally stable up to approximately 1860°C and it is relatively chemically inert. In addition to the use of the encapsulant, volatilization is also suppressed by maintaining an inert gas pressure greater than the pressure of the volatile material on the outer surface of the liquid encapsulant.

The first liquid encapsulated Czochralski GaAs growth was reported by Mullin et. al.[17]. Using a standard Ge Czochralski puller and B_2O_3 as an encapsulant, they were able to grow one [100] GaAs crystal which was completely single as well as one crystal which was semi-insulating. Today, LEC can reproducibly manufacture semi-insulating GaAs up to 4" in diameter;

however, these crystals have a rather large density of structural defects. The need for an improved technique for SI GaAs crystal growth increases with the desire for lower dislocation density crystals that are more homogeneous (i.e. crystals with more uniform electrical properties across the diameter of the wafers).

Aside from pulling from a melt, the other basic means of growing crystals from the melt is directional solidification. Controlled solidification is initiated by producing a temperature gradient to directionally cool the GaAs melt which is in contact with a seed. The freezing interface travels along the length of the boat and the crystal grows in the direction of the seed. This process can be performed using the Bridgman[18], or Stockbarger[19], or the gradient freeze[20] techniques. Schematics of the three systems are shown in figure 3. Any one of these techniques may be set up in either a horizontal or vertical configuration. In the Bridgman technique, a crucible containing the melt is slowly removed from a furnace. The Stockbarger technique is a modification of this: the crucible is moved from a high temperature furnace to a low temperature furnace. Alternately, the furnace(s) may be moved while the crucible remains stationary. Both the Bridgman and Stockbarger techniques have the advantage of permitting independent control of the interface shape, interfacial temperature gradient, and growth rate. In the gradient freeze method, the crucible containing the melt is preferentially cooled from one end. The cooling is achieved by decreasing the temperature of the furnace. The disadvantages of this method include poor control of both the temperature gradient and the growth rate.

LEC produces crystals from which wafers up to 4" in diameter are sliced. There is not much loss of material due to grinding of the ingot to a uniformly circular diameter. A disadvantage of any horizontal technique is that the ingots

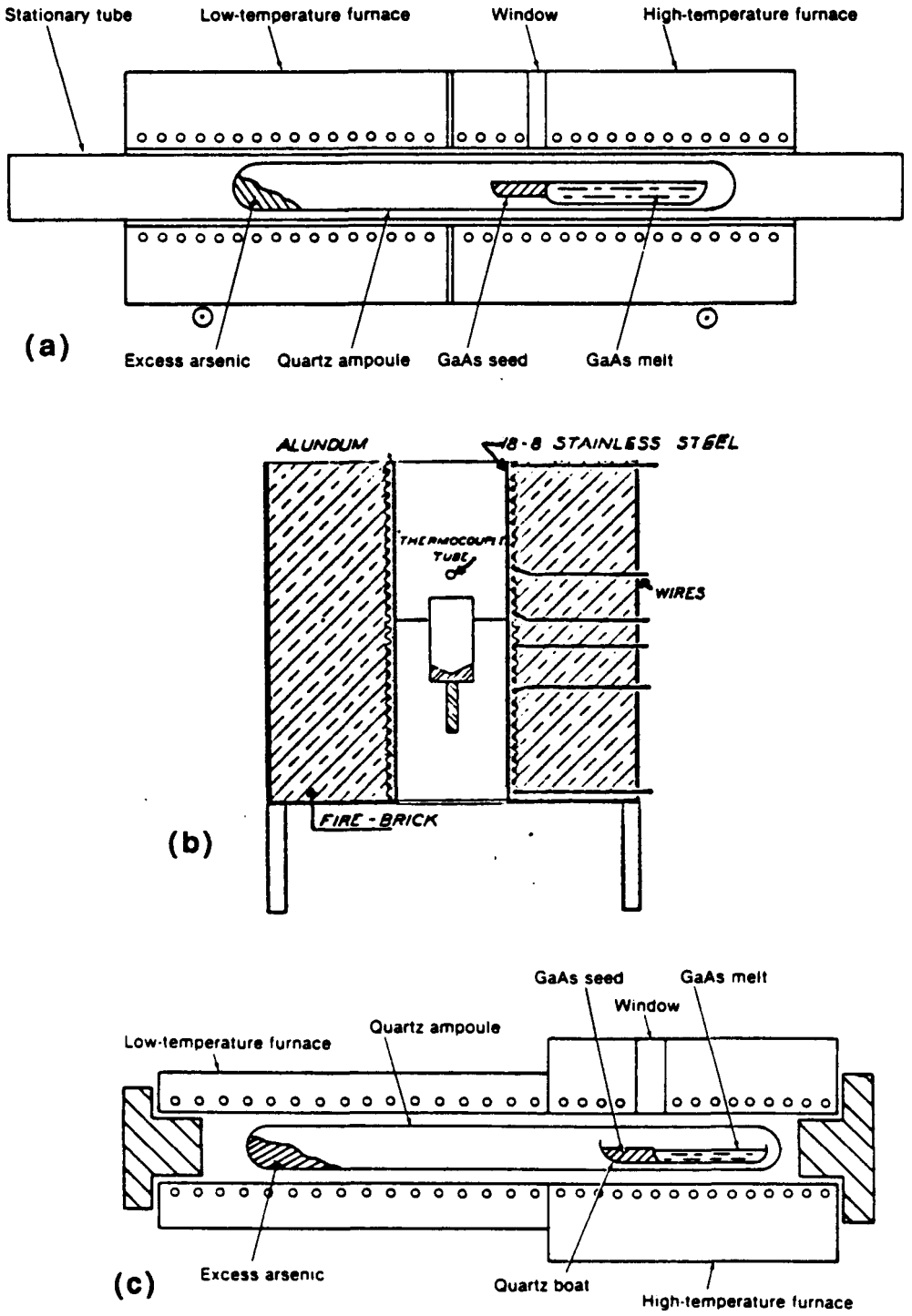

Figure 3. Schematics:(a) a typical horizontal Bridgman system, (b) the original Stockbarger vertical system, and (c) a horizontal gradient freeze system.

acquire the shape of the boat. These are usually half-cylinders leading to the so-called D-shape crystals. HB produces GaAs wafers with a maximum diameter of 2-3". Circular wafers are cut from the D-shape crystals which implies loss of material. This is not the case for vertical techniques. Large diameter, cylindrical crystals can be produced with crucibles that have a cylindrical shape. This is an important point when considering a technique for growing crystals for device applications since most of the wafer production equipment is designed for circular wafers. Also, the loss of costly material due to grinding is minimized.

In the new vertical gradient freeze (VGF) method that was used for this study, directional cooling is achieved through the use of a multizone furnace. This type of furnace provides better growth rate and temperature control since each zone is independently computer-controlled. Stoichiometry control in most directional solidification methods is achieved through an As overpressure maintained by an arsenic source heated in the low temperature zone of the furnace. The technique has been described in detail by Parsey et. al.[21] and Bourret et. al[22]. for growth of GaAs in a horizontal configuration. Recently, Monberg et. al.[23] employed the technique for the vertical growth of InP.

Today's directional solidification techniques impose significantly lower thermal gradients on the melt-solid charge than the CZ technique. These lower gradients result in reduced convective flows and low thermal stresses generated in the crystal. The overall quality of LEC boules is compromised by the large dislocation densities, 10^4-$10^5/cm^2$. HB and VGF crystals have dislocation densities of less than $5000/cm^2$.[24] The best VGF crystals have less than $1000/cm^2$.[25]

The VGF technique combines advantages of both LEC and HB and has the potential to improve the crystalline perfection of bulk crystals, i.e., lower

dislocation density and controlled stoichiometry, in particular. These are a result of the small axial and radial temperature gradients during growth. A few groups have reported on their progress with the new VGF technique.

Chang[26], et. al. showed experimentally and theoretically that it is possible to grow gallium arsenide and napthalene crystals using vertical gradient freeze. They grew the GaAs in a silica crucible which was contained in a sealed quartz ampoule. By controlling the furnace temperature gradient and cooling rate, they were able to control the interface shape and freezing rate. The GaAs crystals were n-type with resistivities of 0.01 Ω-cm and carrier concentrations of 10^{17} cm^{-3}.

The Gault[27] process is a VGF technique employing a PBN crucible with a seed well and a PBN growth vessel, the latter requiring that it be an open system since PBN cannot be sealed under vacuum. A top cap made of hot pressed boron nitride confines the arsenic vapor so that stoichiometry is maintained. There is a loss of arsenic vapor through an annulus between the top cap and the growth vessel; however, sufficient condensed phase arsenic is present in the low temperature zone to maintain the desired partial pressure during growth. Gault et. al. were the first group to report on a seeded VGF process of crystal growth that produced 50 mm diameter GaAs, InP and GaP. Their boules had lower dislocation densities than crystals grown by the alternate methods.

Recently, Clemans, et. al.[28] reported the scale-up of the Gault process for the manufacture of 75 mm diameter, 3 kg undoped semi-insulating GaAs. The crystals had dislocation densities less than 2500/cm^2 and typical room temperature mobilities of 7000 $cm^2/V \cdot s$. The excellent material uniformity resulted in high quality substrates suitable for GaAs integrated circuit manufacture.

The VGF system of Abernathy et. al.[29], is very similar to the system used in this work. It employs a PBN seeded crucible in a sealed silica ampoule with a small amount of As in the low temperature zone of the furnace to maintain the desired As pressure in the ampoule during growth. Thermocouples positioned around the diameter along the length of the system and thermocouples placed radially in each zone control the temperature. The thermal gradient across the full diameter of the melt is <25°C/cm and slightly higher in the cone section of the crucible. This group produced high quality 2" diameter undoped and In-alloyed GaAs with a resistivity of $>10^7$ Ω-cm and dislocation density of 2000 - 6000/cm^2 for the former and 0 - 1000/cm^2 for the latter.

1.3 Silicon Contamination

The key to attaining SI crystals, as stated previously, is to control the balance of donors and acceptors in the material. The major problem with the GaAs growth systems that use quartzware, as is used in this work, is silicon contamination. Si contamination during GaAs growth has been a problem since its discovery in the early 1960's. It results both from the reaction of liquid gallium with the quartz boat and from gaseous chemical reactions at the high growth temperatures, which break down the silica ampoule and hence unintentionally dope the GaAs melt with silicon. The chemistry which is occurring can be described by the following reactions[30]:

(1) 4 Ga (l or g) + SiO_2 (s) = 2 Ga_2O (v) + Si (l)

(2) Si (l) + SiO_2 (s) = 2 SiO (v)

(3) 3 Ga_2O (v) + As_4 (v) = Ga_2O_3 (s) + 4 GaAs (s)

(4) SiO (v) = SiO (s).

Several attempts have been made to eliminate the silicon contamination in crystal growth systems. Standard quartz boats were replaced with nonsilica

boats. Knight[31] reported that the use of carbon or carbonized silica boats in quartz ampoules in the gradient freeze preparation of GaAs results in material that is more strongly n-type than when silica boats are used. He stated that carbon probably enhances the reduction of the silica according to the following reaction:

(5) SiO_2 (s) + 2 C (s) = Si (s) + 2 CO (g).

Stearns and McNeely[32] obtained results similar to Knight's by replacing the silica boat with a boron nitride boat but retaining a silica ampoule. They reported enhanced Si contamination due to the presence of the boron. Kobayashi et. al.[33] showed that in using a PBN crucible in a Bridgman configuration (silica ampoule still present) boron is incorporated into the GaAs melt due to a dissociation of the PBN boat. They further found that the boron in the melt enhances the silicon contamination in GaAs by reacting with the SiO in the growth ambient. The SiO is dissolved in the melt and mixing occurs by convection. They propose that the following chemical reactions occur:

(6) Ga (in GaAs melt) = Ga (g)

(7) 2 Ga (g) + SiO_2 = Ga_2O (g) + SiO (g)

(8) 3 SiO (g) + 2 B (in melt) = B_2O_3 (l) + 3 Si (in melt)

(9) 3 Ga_2O +2 B (in melt) = B_2O_3 (l) + 6 Ga (in melt)

They confirmed this by adding B to the melt and measuring the Si concentration. They established a two-thirds power relationship between the Si and B concentrations which supports the hypothesis that B enhances the Si contamination.

Cochran and Foster[30,34] performed detailed equilibrium calculations which showed that reaction (2), of gallium with silica which produces Ga_2O and Si as stated above, is the controlling reaction responsible for Si contamination. Hence, it is the Ga_2O vapor that is controlling the quartzware reduction.

Consequently, they suggested the use of a capillary tube from the hot end of the growth chamber to the cold end to impede the diffusion of various gaseous species to the cold end. The idea, which was implemented by Kubota and Katsui[35] for InP growth, is that the capillary tube should act as a barrier preventing In_2O vapor (or in the case of GaAs growth, Ga_2O vapor) from diffusing into the lower temperature zone and condensing. If the oxide vapor is kept from the cold end (or at least its flow to the cold end is minimized) then reaction (1), mentioned above, will occur only until the high temperature zone is saturated with Ga_2O vapor. Once this occurs, an equilibrium will be reached, and silica reduction and hence silicon contamination of the GaAs melt will be reduced. The capillary should minimize oxide vapor diffusion. This can be explained by the view that the countercurrent of the group-V element vapor into the high temperature zone effectively reduces diffusion of the metal oxide. Shimoda and Akai[36] used a 3 temperature zone HB set-up, with the middle zone acting as a capillary. Both groups had moderate success with reducing the Si contamination but neither could consistently produce semi-insulating material.

Ainslie et. al.[37] were the first to report that the addition of oxygen to the reaction tube in which GaAs is produced reduces Si contamination. They reported improved electrical properties of the material with 1-10 Torr of oxygen and at 155 Torr their material became semi-insulating. They subsequently concluded that the suppression of the SiO_2 dissociation at the walls of the silica reaction tube was indeed due to the oxygen addition[38]. Others achieved oxygen doping by adding small amounts of gallium oxide or arsenic oxide to the starting material.

Another idea suggested by Cochran and Foster[34] was that the volume of free space in the hot zone of the furnace should be limited since this space is

filled with gaseous reaction products. One of the ways in which this work implements their idea is by placing a cap on the ampoule. The cap is not sealed and it has a small hole to allow As to be in equilibrium with the melt in order to prevent volatilization of the As from the melt surface. In the VGF system, the gas flow by convection is assumed to be dominant over any diffusion process of the gaseous species in the ambient. The cap, therefore, is a physical barrier to transport by convection. It separates the two volumes, above and below the cap, and thus reduces mixing of the gases above and below the cap.

Another means of limiting the volume of free space in the high temperature zone of the furnace that was implemented in this work was to line the wall of the silica ampoule with a PBN tube. In this way, it was thought that the silicon contaminated gas would be confined between the ampoule and the liner, away from the melt. When used in conjunction with the cap, the amount of free space where the vapors can react with the ampoule was thought to be minimized even further.

Liquid encapsulation practically eliminates the contact of the melt with vapor in the ambient. It was first combined with Vertical Gradient Freeze by Blum et. al.[39] for GaP growth. The LE-VGF grown GaP crystals were easier to grow and a had lower dislocation density than LEC grown GaP. Recently, Monberg et. al.[23] reported the growth of undoped single crystal InP using dynamic gradient freeze with a B_2O_3 encapsulant. Their system contains a modified EDG vertical furnace with 23 zones and is capable of withstanding the high pressure necessary for InP growth.

Another advantage of the B_2O_3 encapsulant is its ability to getter undesirable impurities. Thus, some purification of the melt is achieved through reactions analogous to those proposed by Cochran and Foster[34] for the Ga_2O_3-

melt interaction. The gettering properties of B_2O_3 were first recognized by Goetzberger and Schockley[40]. They found that metal precipitates could be removed or prevented by gettering from surface layers on Si p-n junctions. Mullin et. al.[17] stated that the ability of liquid B_2O_3 to getter foreign metallic oxides and effectively complex the boron and its impurities could be an important property in the preparation of other high purity compounds.

Terashima et. al.[41] proved that the encapsulant has gettering properties during LEC GaAs crystal growth. Prior to the pulling process, the melt was purified in-situ with a bubbling distillation technique. B_2O_3 with a very low water content (<100 ppm H_2O) was used as the encapsulant material. An abrupt decrease in the high Ar pressure inside the growth chamber created bubbles in the molten B_2O_3 encapsulant. They reproducibly correlated the purification of the melt with the amount of electrical conducting current that could pass through the melt. They proposed that the distillation evaporates some impurities such as Si in a form of gaseous compounds from the GaAs melt with minimal As evaporation. All crystals grown with the distillation technique, whether in PBN or SiO_2 crucibles, were semi-insulating and had relatively low Si concentrations. Those grown without in-situ purification showed higher Si concentrations and low resistivities.

1.4 Description of Project

This work concentrates on the development of a new process to grow SI GaAs crystals with a VGF system that contains quartzware. As was described previously, many methods have been used to control Si contamination, the major hurdle preventing reproducible growth of SI crystals; however, the results have often been inconsistent from one study to another. Therefore a systematic study of these methods has been conducted by applying them to GaAs growth

by the VGF technique. The methods include the use of different boat materials, a capillary tube, addition of Ga_2O_3, the use of a BN cap on the crucible, a PBN ampoule liner and B_2O_3 encapsulation. Crystals grown using the above methods are characterized using both room temperature and variable temperature Hall effect measurements, secondary ion mass spectroscopy (SIMS), deep level transient spectroscopy (DLTS) and Local Vibrational Mode Spectroscopy (LVM).

2. EXPERIMENTAL PROCEDURE

All crystals analyzed in this work were grown in a vertical gradient freeze configuration designed to fit Mellen Electro-dynamic gradient (EDG) furnaces[42]. These furnaces are capable of imitating the heat flow characteristics of the Bridgman-Stockbarger or gradient freeze techniques but do not require motion of either the containment vessel, the ampoule, or the furnace. The furnaces which require motion are disadvantageous because they require a long heater core, an extended support apparatus and long growth ampoules. Since they are designed for temperature stability, they are limited in dynamic response. In addition, the number of thermal profiles that they are able to generate is limited by the small number of control zones[21]. In the EDG furnaces, the heating element subassemblies are configured into zones which can be controlled independently. The narrow heating zones are used to shape the axial temperature gradient along the furnace axis. They are micro-processor controlled so that they can be programmed to translate or modify the axial temperature profile in time as the growth proceeds. The design of this furnace was described in detail by Parsey and Thiel[21].

2.1 GaAs Synthesis

For GaAs synthesis, 7N pure gallium (Alusuisse/Alcan) is placed in either a silica or PBN boat at one end of the ampoule and 6N double-refined (Cominco) arsenic is placed at the opposite end of the ampoule. There is a constriction between these two sections of the ampoule so that an alumina ring can be placed between them to help insulate the low temperature zone from the high temperature zone. The ampoule is evacuated and backfilled with N_2 gas three times (to insure that all air is removed from the system) and then is pumped down to a pressure of 1×10^{-5} Torr and sealed. Once loaded, the ampoule is placed in an EDG furnace which is in a horizontal configuration. After heat-up, an equilibration time chosen to be 120 minutes occurs. It has been found that a temperature of 617°C in the arsenic containing section of the furnace produces the optimum As pressure (0.976 atm) for stoichiometric growth[43]. The arsenic is transported in the vapor phase to the gallium, which is held at 1238°C, and the two react to form GaAs. The synthesized material is then slowly cooled. The whole synthesis process takes about 24 hours. A schematic of a synthesis ampoule and synthesis temperature profile are shown in fig. 4.

The GaAs starting material (the charge) used to grow the crystals for this work was one of two sources: undoped semi-insulating M/ACOM material grown by LEC, which is characterized by a carrier concentration of mid 10^7 cm^{-3} and a resistivity of 10^8 Ω-cm, or material that is synthesized in our laboratory in a horizontal gradient freeze system. This material is typically synthesized at an arsenic source temperature of 620°C in a pyrolytic boron nitride (PBN) or quartz boat. Although undoped, the synthesis material is n-type with a free carrier concentration of mid 10^{15} cm^{-3}. The use of two different starting materials is significant because they are produced by different techniques and hence,

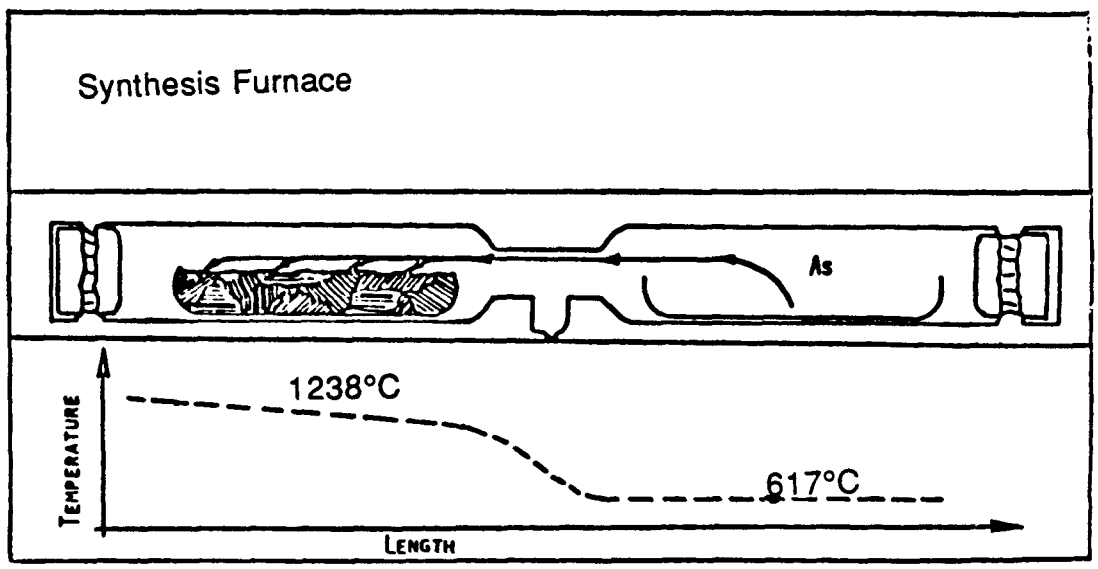

Figure 4. A schematic of the GaAs synthesis ampoule and corresponding temperature profile.

contain different impurities. LEC material generally contains on the order of 10^{15} to 10^{16} cm^{-3} carbon, due to the graphite heating elements in the CZ system, and 10^{17} cm^{-3} boron due the B_2O_3 encapsulant and the PBN growth vessel. These impurities are two to three orders of magnitude less for directionally solidified material[10].

2.2 Crystal Growth

Preparation for growth involves several major steps which I will briefly discuss. The crucible treatment prior to growth is an important process. The quartz crucibles and boats are sandblasted with coarse SiC grit to achieve a rough surface to prevent wetting[44]. They are subsequently cleaned with methanol and de-ionized (DI) water to remove all of the SiC grit and etched with aqua regia (HCl: HNO_3, 3:1 in volume). After a thorough rinse with DI water, they are oven dried in N_2 at 400°C for one hour. Pyrolytic Boron Nitride (PBN, "Boralloy" manufactured by Union Carbide) crucibles are etched with aqua regia, rinsed in boiling DI water, oven-dried in an atmosphere of O_2 and N_2 at 650°C for 1-2 hours and vacuum baked at 1000°C at a pressure of 10^{-5} Torr for 2 hours in order to remove any moisture, volatile suboxides, or carbonaceous materials. The quartz ampoules for both synthesis and growth are cleaned by rinsing them with dilute HF and DI water for 5 to 10 minutes.

Before the seed and charge are loaded into the crucible for growth, they are etched in aqua regia and dried under heat lamps to remove any excess moisture. A <100> seed is positioned in the seed well of either a sand-blasted quartz or PBN crucible. Subsequently, the charge is loaded in the crucible with dopants and encapsulants, such as Ga_2O_3 and B_2O_3, if desired. The crucible is loaded into the tapered part of the large diameter section of the ampoule. A few grams of arsenic are put in the reduced diameter section of the ampoule which

extends into the low temperature zone of the furnace. The ampoule is evacuated to a pressure of $1x10^{-5}$ Torr, sealed with a quartz cup and loaded into the furnace. A schematic of the VGF ampoule and crucible are shown in figure 5a and the temperature profile for growth is shown in figure 5b.

The growth furnace is a 3-inch Mellen EDG furnace configured vertically. It has twelve controlled zones, each with its own sensing thermocouple inserted radially to make contact with the growth ampoule. Ten of the thermocouple positions are shown in fig. 5a. The first zone of the low temperature section of the furnace is used as a buffer, and its thermocouple sits at the bottom of the ampoule. This section is kept at 617°C for the growth. This temperature has been reported to produce a minimum dislocation density in HB GaAs[45]. Also, as previously mentioned, this temperature produces the optimum arsenic pressure for stoichiometric growth in HB systems. Initially, the melt temperature is carefully adjusted to cause a slight melt-back of the seed crystal so that the melt and the seed are in intimate contact. This ensures that the crystal will take on the desired growth orientation. The GaAs growth temperature at the interface is 1238°C. The temperature gradients across the interface are programmed to be 10°C/cm for the solid and <1°C/cm on the liquid side. However, the temperature gradient at the interface is slightly varied in order to keep the growth rate constant. The growth rates vary from 3-5 mm/hr for the various runs discussed below.

During both the heat-up and the cool-down, the As source temperature is gradually ramped with the melt temperature in order to help maintain stoichiometry. The equilibration time for growth is 240 minutes. This long equilibration time is necessary to assure homogeneity of the melt. Slow cooling is important for minimum stress in the crystal. The cooling rates used are 1°C/min down to 900°C and 2°C/min from 900°C to room temperature. This

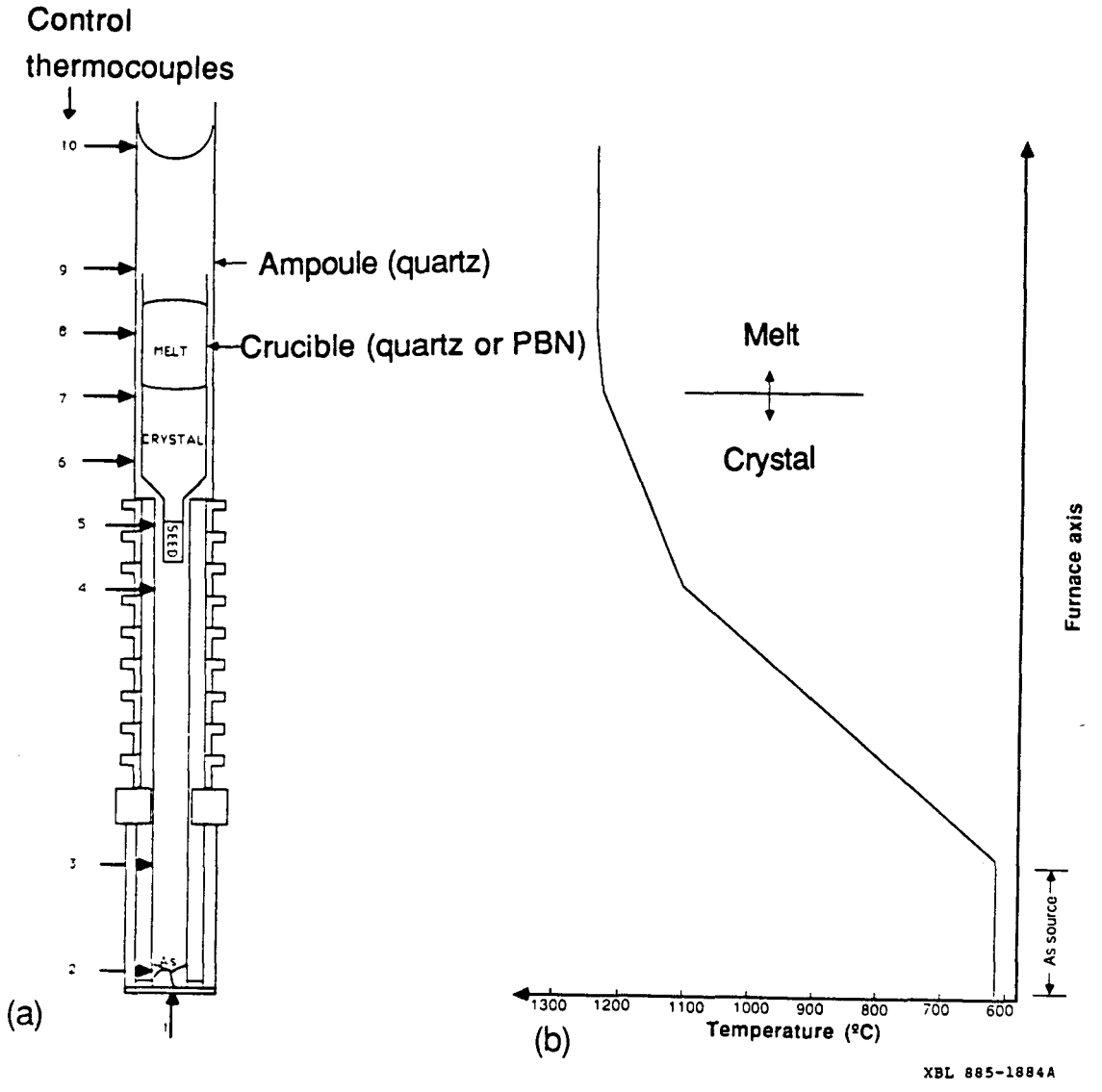

Figure 5. (a) Schematic of the experimental set-up showing the growth ampoule, crucible and position of the control thermocouples. (b) Temperature profile as measured on the outside of the growth ampoule during growth.

allows for the production of very low dislocation density material (less than 2000/cm^2).

2.3 Synthesis Experiments

In an early attempt to eliminate Si from the starting material, syntheses were performed in different boat materials at different As source temperatures. The boats used were either silica, PBN, CVD BN-coated quartz or BN-spray coated quartz. The source temperatures ranged from 617-635°C, which corresponds to arsenic pressures from 0.976-1.4 atm. The high temperature zone was maintained at 1238°C for all the syntheses. It is known that silica boats dissociate during synthesis as discussed in Chapter 1. It was hoped that coating the quartz with boron nitride would prevent the dissociation of the silica. The coating by chemical vapor deposition was done with a system in our laboratory. The Combat Boron Nitride Coating supplied by Standard Oil Engineered Materials required several layers to be sprayed on in order to fully coat the boat. The goal of these experiments was to compare the silicon and free carrier concentrations of the GaAs synthesized in the different boat materials. These syntheses will be referred to by the boat and arsenic source temperature, for example, PBN 617°C implies the material that was synthesized in a PBN boat with an arsenic source temperature of 617°C.

Another idea was to try to purify the starting material that we synthesize in our own laboratory. Several syntheses were performed with Ga_2O_3 added to the gallium in the PBN boat so that the Si concentration in this material would be less than normal, i.e. mid 10^{15} - 10^{16} cm^{-3}. These syntheses were subsequently used for growth. They have low carbon and boron concentrations compared to the SI LEC material from M/ACOM.

2.4 Growth Experiments

Thirteen crystal growth runs were conducted in a systematic way in order to attain SI GaAs crystals. The main characteristics of each run are listed below in table I. Runs V29, V36, V37 and V43 were not included in the table below because they were not part of this project .

Table I. VGF Crystal Growth Run Conditions

RUN	CRUCIBLE	CHARGE	ADDITIONS
V28	quartz	SI M/ACOM	capillary tube
V30	quartz	quartz 620°C	capillary tube
V31	PBN	SI M/ACOM	BN cap
V32	PBN	SI M/ACOM	BN cap, Ga_2O_3
V33	PBN	SI M/ACOM	B_2O_3 encapsulant
V34	PBN	PBN 620°C	BN cap, Ga_2O_3
V35	PBN	PBN 620°C	BN cap
V38	PBN	SI M/ACOM	PBN liner, BN cap
V39	PBN	SI M/ACOM	B_2O_3 encapsulant
V40	PBN	PBN 620°C (Ga-rich)	BN cap, Ga_2O_3, increased As pressure
V41	quartz	SI M/ACOM	B_2O_3 encapsulant
V42	PBN	SI M/ACOM	B_2O_3 encapsulant, In doping
V44	PBN	Ga_2O_3 PBN 620°C	B_2O_3 encapsulant

The two runs in which we used a capillary tube, V28 and V30, employed specially designed ampoules that allowed for the placement of a capillary just below thermocouple #4 (see fig.6). The tube has a 2 mm I.D. and is 20 cm in length. Using data from Cochran and Foster[30] and Kubota and Katsui[35], it was determined that the top of the capillary tube must be above 938°C for synthesis and 942°C for growth in order for it to be effective in preventing Ga_2O from condensing out and thus preventing the reduction of the Si ampoule as discussed in chapter 1. The temperature difference for synthesis and growth is

due to the different As source temperatures for the two separate processes, 620°C for the synthesis and 617°C for growth.

In addition to the capillary, V30 was grown with a charge which was synthesized in silica rather than PBN. The idea behind this was to see if removing all BN from the system would have any effect on the silicon concentration since it has been shown that B enhances the Si contamination, as discussed in Chapter 1.

V31 was the first crystal growth run in which we employed a hot-pressed BN cap on the PBN crucible. The purpose of the cap was to limit the free space above the crucible where gaseous chemical reactions occur. The cap had a 1 mm in diameter hole in its center so that arsenic vapor could remain in equilibrium with the melt to prevent volatilization of the arsenic. In many of the subsequent runs, we used a cap.

V32 is the run in which we initiated the addition of Ga_2O_3 to the melt. The amount of Ga_2O_3 added to any growth run in which it is listed in Table I is 1.5×10^{-4} times the charge weight. This value was determined by Yong to be the minimum amount necessary to achieve semi-insulating material in horizontal gradient-freeze[46]. These two runs, V31 and V32, used the SI M/ACOM material as the charge. They were repeated as V35 and V34 with the same conditions except the PBN 620°C charge was used to see if the starting material impurities had any effect on the final characteristics of the crystal.

The first run in which we used a B_2O_3 encapsulant, V33, was unseeded. The purpose of the encapsulant was to improve the crystal quality by restricting direct contact between the crucible and the melt. The encapsulant might also serve as an alternative to the BN cap and its gettering ability would prove quite useful for elimination of silicon. V39 was a repeat of this run except that it was seeded.

The increase of EL2 concentration with the increase in arsenic source temperature was first reported by Holmes[11]. Since it is known that EL2 is important for semi-insulating behavior, V40 was grown with an increased As pressure to increase the EL2 concentration and consequently produce SI GaAs. The charge used for the V40 run was Ga-rich. This is important to note because it could have an effect on the final product.

In V38 PBN liner was used. The liner was 25 cm in length and fit over the crucible such that it lined the ampoule wall in the growth section of the ampoule. Additions such as the PBN liner, the capillary tube, and BN cap for the crucible are shown in a schematic in figure 6.

V41 was a crystal grown in a quartz crucible with a B_2O_3 encapsulant. V42 was a repeat of V39 with In doping in order to see striations in the crystal, and a faster growth rate. This run was also important to demonstrate that we could reproducibly produce SI material. V44 used the oxygen-doped starting material in order to see if we could achieve semi-insulating crystals with our own charge.

2.5 Characterization

The main characterization technique used to analyze all charge materials and crystals in this work was the Hall effect. A Hall set-up with a van der Pauw[47] sample geometry and a 3kG magnetic field was employed. Room temperature Hall resistivity measurements were performed to determine the carrier concentration and mobility of each crystal. With variable temperature Hall effect measurements, a plot of the natural log of the carrier concentration versus inverse temperature can be obtained. Since the concentration $n = n_0 \exp(-E_a/kT)$, where n_0 is a constant, k, the Boltzmann constant and T, the temperature, the slope of the freeze-out curve gives the binding energy of the

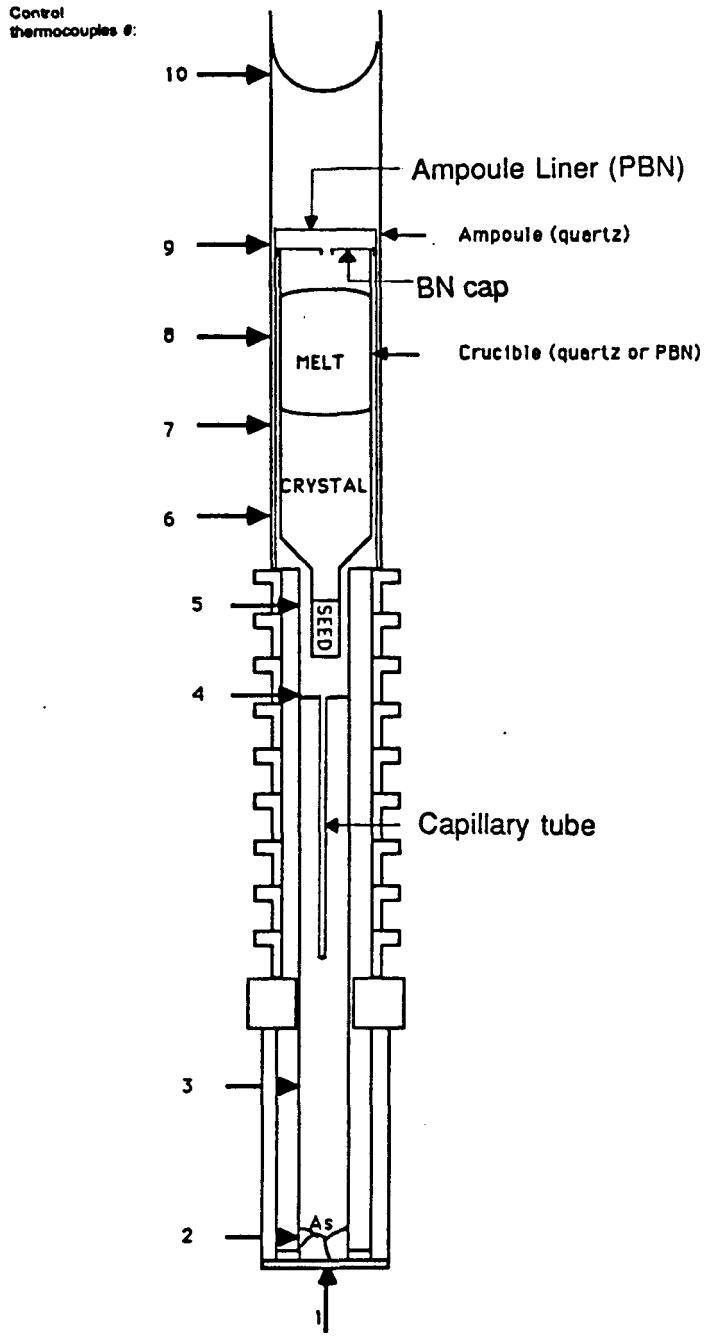

Figure 6. Silicon contamination control additions: the BN cap, the PBN liner and the capillary tube.

dominant donor or acceptor level in the material (for compensated material). This defect or impurity level can often be identified by its energy.

For sample preparation, wafers were cut about 1-inch apart down the length of the crystal and 6x6x1 mm^3 samples were prepared using the following procedure. The samples were hand-lapped with 6 μm alumina, etched in HCl and polish-etched for 2-3 minutes in H_2SO_4:H_2O:H_2O_2 (3:1:1) . In-Sn contacts were pressed onto the four corners and alloyed at 400°C for 10 min. in an argon atmosphere. Copper wires dipped in indium were pressed onto the In-Sn contacts.

Local Vibrational Mode Spectroscopy (LVM) was used for several crystal samples in order to determine the concentration of carbon on arsenic sites, where it is predominantly observed. With LVM, only impurities atoms lighter than the host atoms can be determined since their vibrational frequencies depend on the square root of the coupling constant divided by the mass. Impurity atom frequencies need to be higher than lattice frequencies in order for them to produce sharp absorption bands called Local Vibrational Modes (LVMs)[48]. LVM spectroscopy measures the optical absorption by resonating bonds between the carbon impurity sitting on an As site and the surrounding Ga atoms. The carbon concentration is related to the area under the peak generated by the impurity in a plot of absorption coefficient, α, versus wavenumber. The height of the peak is α and the width of the peak is Δ. The calibration of Hunter et. al.[49] and Brozel et. al.[50] gives $\alpha \cdot \Delta = 1$ cm^{-2} for a carbon concentration 10^{16} cm^{-3} in GaAs was used in this work. This value is accurate within ± 15%.

The C_{As}, carbon on As site, peak occurs at 582.4 ± 1 cm^{-1}. Theis et. al.[51] measured the LVM band of ^{12}C under high resolution conditions and found splitting of the band into five levels. The bands arise from the carbon on As

sites with different nearest-neighbor configurations of the Ga isotopes. The C_{As} acceptor has four nearest-neighbors and Ga has two isotopes with masses of 69 and 71. A number of different mode frequencies result from the different isotopic arrangements on the four nearest neighbor sites.

Secondary Ion Mass Spectroscopy (SIMS) was used to determine the Si concentration in select crystals. SIMS is a technique in which an ion beam, incident upon a sample, causes atoms and molecular complexes to be sputtered from the surface. Some fraction of the sputtered material will escape as ions depending upon the energy of the beam and its angle of incidence. These scattered ions (i.e. secondary ions) are collected in a mass spectrometer for mass-to-charge ratio separation and detection. They are representative of the composition of the sample[52]. By comparison of the ratios of the ion yields of the sample to the ion yields of standard samples, the concentrations of impurities in the material can be determined.

SIMS is a technique which can be used for depth profiling, imaging or bulk analysis. When it is used for bulk analysis, as was the case in this work, the sensitivity is maximized by the use of a high sputtering rate on a small rastered area. It gives a measurement of the average composition of a sample. With standards, accuracy is greatly improved. Detection of trace and ultra-trace impurities is possible. In general, the detection limit of impurities in GaAs lies between the ppm and ppb levels.

Samples for LVM and SIMS were lapped with 3 μm Al_2O_3 and mechanically-chemically polished with a 1:1:1 solution of syton (a silica emulsion):H_2O_2:H_2O.

Deep Level Transient Spectroscopy (DLTS) was performed on early crystals to determine the deep levels present in our VGF crystals. DLTS is used to obtain information about impurity levels in the depletion region of a Schottky

barrier by observing the capacitance transient associated with the return to thermal equilibrium of the occupation of the levels following an initial nonequilibrium condition, i. e. a bias pulse. The time constant of the transient as a function of temperature is measured and from this the activation energy can be obtained. The technique displays the spectrum of traps in a crystal as positive or negative peaks (depending whether the level is near the conduction band or valence band) as a function of temperature. The height of the peak is proportional to the trap concentration and the position of the peak, in temperature, is uniquely determined by the thermal emission properties of the trap[53]. DLTS samples were lapped and polish-etched with 3:1:1. Evaporated Au-Ge and Au contacts formed the ohmic and Schottky contacts, respectively, on the samples. The Au-Ge contacts were annealed for 10 minutes at 450°C in an argon atmosphere.

3. RESULTS and DISCUSSION

3.1 Syntheses

The initial syntheses that were performed to compare the use of silica and PBN boats at different As source temperatures confirm that Si contamination is indeed due to a vapor transport mechanism. A plot of the average free carrier concentration, n, versus arsenic source temperature is shown in fig. 7. For both the silica and PBN boats, there is a slight increase in carrier concentration as the source temperature increases. An increase in the source temperature corresponds to an increase in the As pressure in the growth environment. The higher pressures cause more collisions of the atomic species in the gases with the atoms in the melt. This results in an increase in Si

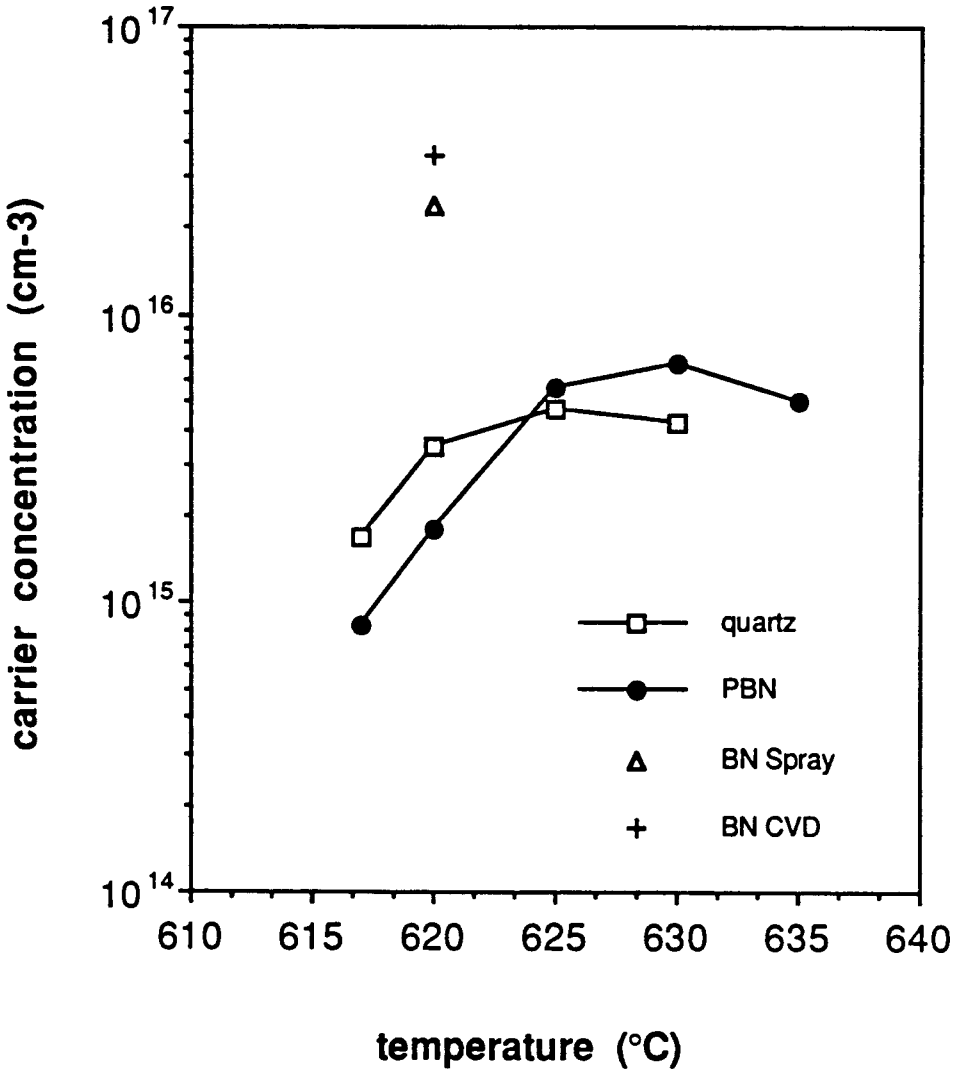

Figure 7. Average carrier concentration versus arsenic source temperature for various GaAs syntheses.

contamination which in turn leads to an increase in the free carrier concentration. These results confirm the vapor transport mechanism of Si contamination. Also, it is observed that for our horizontal gradient freeze (HGF) syntheses, there is little difference in carrier concentration between using a silica or a PBN boat.

The BN coated quartz boats, both the BN sprayed and the BN CV deposited, had an average carrier concentration that was an order of magnitude higher than the regular quartz or PBN boats. This is probably due to other impurities present in these coatings. It has been reported[54] that the CV deposited BN films have a low density structure. This turns them into an important source of boron to dope the GaAs melt (probably a greater source than PBN) since they have more surface area. Thus the increased carrier concentration in this synthesis may be a result of the extra boron present, which can enhance silicon contamination, as discussed previously. It is also noted that the impurities in the BCl_3 source gas used in the CVD coating process and the decomposition of the silica parts that were used in the CVD system may add to the silicon impurity concentration in the material synthesized in the CVD BN quartz coated boat.

SIMS data of the 620°C quartz and PBN syntheses show Si concentrations of 6×10^{15} cm^{-3} and 1×10^{16} cm^{-3}, respectively. These differ by less than a factor of 2 which lies within the error of the measurements. Thus, one cannot conclude that there exists a real difference in these two processes. The detection limit for Si in GaAs is 10^{14} cm^{-3}. The SIMS results for other impurities are shown in Table II. It can be seen that in both the synthesis material and the early VGF crystals, the amount of other possible donors, such as Se and Te are negligible and hence, one is more confident in calling silicon the main donor impurity present in the material. The concentration of the

acceptor Sn is also quite small. The detection limits for C and O by SIMS are higher than the residual concentrations of these impurities in our crystals. Therefore, we only quote upper limits.

Table II. Concentration of impurities as determined by SIMS.*

SAMPLE	CONCENTRATIONS (cm^{-3})				
	C	O	Se	Sn	Te
Q-620	$\leq 2x10^{16}$	$\leq 4x10^{16}$	$\leq 2x10^{12}$	$\leq 2x10^{14}$	$\leq 6x10^{12}$
PBN620	$\leq 2x10^{16}$	$\leq 3x10^{16}$	$\leq 5x10^{12}$	$\leq 7x10^{13}$	$\leq 1x10^{13}$
V18	$\leq 3x10^{16}$	$\leq 3x10^{16}$	$4x10^{13}$	$\leq 2x10^{14}$	$\leq 1x10^{13}$
V20	$\leq 2x10^{16}$	$\leq 4x10^{16}$	$\leq 2x10^{13}$	$\leq 2x10^{14}$	$\leq 9x10^{12}$

*SIMS performed by Charles Evans and Associates.

From previous work[25], it was determined that more silicon is being incorporated into the crystal during growth when a silica crucible is used than when a PBN crucible is used. The two crystals, V18 and V20, grown in silica and PBN crucibles respectively, were also analyzed by SIMS. It was found that the former had 2×10^{17} cm^{-3} Si, while the latter had 2×10^{16} cm^{-3}. Both of these crystals used a PBN 620°C charge as starting material. The carrier concentration of these samples was 1×10^{17} cm^{-3} and 4×10^{16} cm^{-3}, respectively. Thus it can be seen that the free carrier concentration correlates fairly well with the silicon concentration in VGF crystals grown without any method to prevent decomposition of the silica crucible or ampoule.

By adding 1.5×10^{-4} times the charge weight Ga_2O_3 to the PBN boat that holds the gallium for synthesis, the carrier concentration of the synthesized material was reduced an order of magnitude. This is probably due to the role that the oxide plays in preventing the silica ampoule dissociation according to the equations discussed in chapter 1:

(1) 4 Ga (l or g) + SiO_2 (s) = 2 Ga_2O (v) + Si (l)

(3) 3 Ga_2O (v) + As_4 (v) = Ga_2O_3 (s) + 4 GaAs (s).

Parsey[43] showed the decrease in silicon and free carrier concentrations with the increase of Ga_2O_3 weight fraction for silicon doped HB-grown crystals. He reported significant reductions in silicon concentration but smaller reductions in the free carrier concentration.

For our syntheses, the results were significantly improved by adding a larger weight fraction of gallium oxide, 7.5×10^{-4}. The carrier concentration was reduced to 3×10^{11} cm^{-3}. Single crystal pieces of this material had very good mobility, 6000-6400 $cm^2/V \cdot s$. Even more Ga_2O_3, 1×10^{-3} weight fraction, produced material with nearly the same carrier concentration as the previous synthesis. Thus, the data show that there is a saturation effect occurring to prevent further purification. A plot of the carrier concentration versus weight fraction of Ga_2O_3 is shown in figure 8.

3.2 Growth Results

Of the thirteen GaAs crystals grown in this work, all are n-type and two are semi-insulating. In the systematic approach to produce SI material and control the silicon contamination, a group of crystals which span a wide range of carrier concentrations (10^7 -10^{17} cm^{-3}) and resistivities (10^{-3} - 10^8 $\Omega \cdot cm$) have been produced. The carrier concentration range and resistivity range between the seed end and the tail end of each crystal are shown in Table III.

Table III. Average Carrier Concentration and Resistivity of Crystals

CRYSTAL	CARRIER CONCENTRATION RANGE (cm^{-3})	RESISTIVITY RANGE ($\Omega \cdot cm$)
V28	7.0×10^{16} - 8.3×10^{17}	0.069 - 0.004
V30	1.2×10^{17} - 8.5×10^{17}	0.025 - 0.003
V31	2.3×10^{13} - 7.7×10^{16}	3610 - 0.089
V32	2.4×10^{13} - 5.2×10^{15}	1130 - 0.20
V33	1.7×10^{10} - 3.5×10^{14}	3.1×10^5-6.0

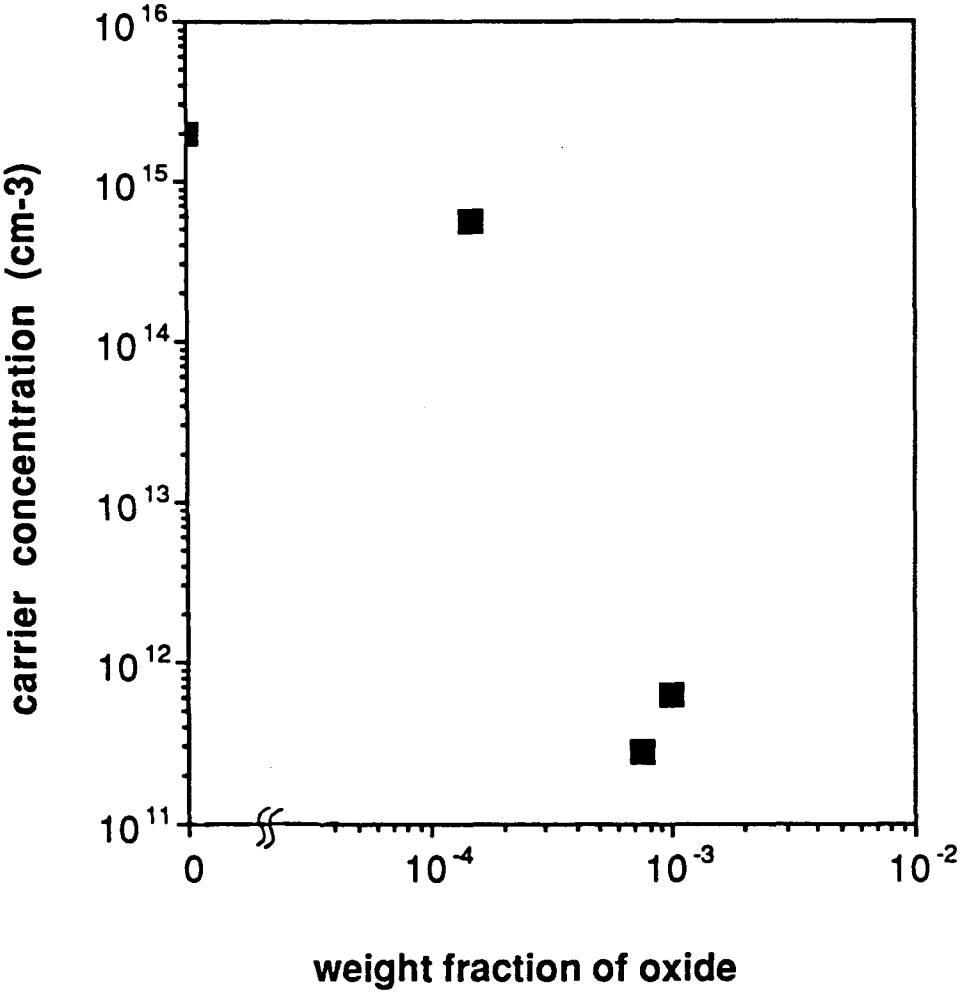

Figure 8. Average carrier concentration of syntheses versus gallium oxide weight fraction.

V34	1.7×10^{11}	$- 3.7 \times 10^{13}$	$2.5 \times 10^{4} - 210$
V35	4.0×10^{13}	$- 2.3 \times 10^{17}$	1300 - 0.075
V38	1.6×10^{15}	-3.2×10^{16}	168 - 0.04
V39	6.0×10^{6}	$- 3.2 \times 10^{15}$	$2.7 \times 10^{8} - 0.4$
V40	$4\ 6 \times 10^{13}$	$- 1.1 \times 10^{15}$	3900 - 46
V41	3.2×10^{14}	$- 6.4 \times 10^{14}$	4.5 - 2.2
V42	5.6×10^{6}	$- 1.4 \times 10^{8}$	$3.2 \times 10^{8} - 8.9 \times 10^{6}$
V44	1.2×10^{9}	$- 1.6 \times 10^{10}$	$2 \times 10^{6} - 4.3 \times 10^{5}$

It appears that SI crystals can only be produced by total liquid encapsulation. More detailed results for the semi-insulating crystals V39 and V42 are given in Table IV. The resistivities and mobilities along the length of each crystal are shown in Table IV. The location in the crystal is given by the value of the fraction solidified, which is referred to as g.

Table IV. Resistivities and Mobilities of the SI crystals.

CRYSTAL	LOCATION	MOBILITY	RESISTIVITY
	g	($cm^2/V \cdot s$)	($\Omega \cdot cm$)
V39	0.16	3200	2.0×10^{8}
	0.48	3800	2.7×10^{8}
	0.56	2350	1.7×10^{7}
	0.74	4700	0.4
V42	0.29	3500	3.2×10^{8}
	0.57	5500	4.1×10^{7}
	0.86	5200	8.9×10^{6}

It should be noted that the mobilities and resistivities of these crystals are comparable to some reported in the literature for VGF material. Gray et. al.[55] reported VGF-grown GaAs crystals with average mobilities of 5400-5900 $cm^2/V \cdot s$ and ranging between 3100-6100 $cm^2/V \cdot s$ and resistivities in the mid $10^7\ \Omega \cdot cm$. As mentioned in Chapter 1, Clemans et. al.[27] reported the growth of high resistivity material with slightly better mobilities (7000 $cm^2/V \cdot s$). Low-angle

grain boundaries and arsenic precipitates may be limiting the mobility in our crystals. Improvements in the structural perfection of the crystals through optimization of the growth parameters is underway and should result in an increase in the mobility of our VGF-grown GaAs crystals.

The accumulation of impurities near the end of the crystals, caused by segregation, leads to an increase in the carrier concentration. This results in a reduction of the resistivity as shown in Table III.

3.2.1. Role of the Capillary Tube

The capillary tube, acting as a diffusion barrier, minimizes the diffusion of Ga_2O vapor to the low temperature end of the ampoule. The countercurrent of As vapor into the high temperature zone of the furnace should reduce the diffusion of the metal oxide into the cold end of the furnace. As a result, the decomposition of silica is minimized because the high temperature zone becomes saturated with Ga_2O and decomposition should cease according to the following reaction:

(1) 4 Ga (l or g) + SiO_2 (s) = 2 Ga_2O (v) + Si (l).

The capillary tube proved ineffective in the VGF system for preventing silicon contamination. It can be seen above that the crystals V28 and V30 had very high carrier concentrations and low resistivities. The concentrations were no lower than the concentrations of crystals grown without any means for preventing Si contamination. Also, removing all the BN from the system, to insure that boron could not enhance the silicon, did not seem to have any effect. It should be noted that during the growth of V30 a coldspot occurred in the low temperature zone of the ampoule where some arsenic condensed during growth. Low arsenic temperatures (< 617°C) correspond to lower As pressures and cause some volatilization of the As during growth. Thus, the stoichiometry

deviates toward gallium-richness. Hence, V30 may be Ga-rich. It is difficult to draw any specific conclusions from these results since it is not known how extra gallium affects silicon incorporation during growth. V28, however, did show the capillary tube to be ineffective in our system. This is probably because convective flows rather than diffusion are the dominant gas flow mechanism in the VGF system. Thus minimizing diffusion is insufficient for preventing silica ampoule reduction.

3.2.2. Role of PBN Cap and Ampoule Liner

The use of the hot-pressed BN cap on top of the crucible, to limit the contact between the ambient and the melt and reduce transport of contaminated gases by convection, reduced the free carrier concentration one-half to one order of magnitude from runs with no precautions against silicon contamination. This can be seen by comparing the results of V20 with those of V31 and V35 in Table V. The cap was not fully efficient in eliminating silicon contamination, probably because it did not act as a complete barrier to isolate the Si-contaminated vapors from reacting with the melt surface.

Table V. Comparison of crystals grown with and without BN cap

CRYSTAL	AVERAGE CARRIER CONC (cm^{-3})
V20	1×10^{17}
V31	2×10^{16}
V35	5×10^{16}

The PBN tube was used to line the ampoule walls in order to confine the convective cells of silicon contaminated gas between the ampoule and the liner, and thus away from the melt. It had an effect similar to that of the cap; it did help reduce the Si contamination to some extent but it did not offer enough

prevention so that semi-insulating material could be achieved. The average free carrier concentration of V38, which used the ampoule liner and the BN cap, was 1.4 x 10^{16} cm^{-3}, only slightly lower than V31, in which we employed the cap alone. Thus, one can conclude that limiting the volume of free space in the hot zone of the furnace so that gases that react with the nearby silica are not in direct contact with the melt did work to some extent. However, it was not sufficient enough in controlling the silicon contamination in our system in order to produce SI material.

3.2.3 Effect of Ga_2O_3 addition

As has been shown by several authors, oxygen doping by the addition of Ga_2O_3 to the growth ampoule, can be used to reduce silicon contamination. The reactions occurring in the ampoule, as stated previously, are:

(1) 4 Ga (l or g) + SiO_2 (s) = 2 Ga_2O (v) + Si (in melt)

(2) Si (in melt) + SiO_2 (s) = 2 SiO (v)

(3) 3 Ga_2O (v) + As_4 (v) = Ga_2O_3 (s) + 4 GaAs (s)

(4) SiO (v) = SiO (s).

The addition of Ga_2O_3 pushes reaction 3 to the left, producing more Ga_2O vapor. This, in turn, pushes (1) to the left and thus prevents the dissociation of SiO_2.

Ga_2O_3 proved to be effective in reducing the silicon contamination in our system. This can be seen clearly from the reduced carrier concentrations of V32 and V34 as well as from the synthesis results stated previously. However, it is interesting to note that the Ga_2O_3 was much more effective in preventing silicon contamination in the crystal grown with our charge than the crystal grown with the M/ACOM charge. Purification equivalent to a one order of magnitude reduction in the carrier concentration was observed when comparing V31 to

V32, whereas purification equivalent to over three orders of magnitude comparing V35 to V34. This can be seen directly by comparing the average carrier concentrations for the various crystals shown in Table VI.

Table VI. Comparison of crystals grown with and without Ga_2O_3.

CRYSTAL	OXIDE	CHARGE	AVERAGE CARRIER CONC. (cm^{-3})
V31	NO	M/ACOM	2×10^{16}
V32	YES	M/ACOM	2×10^{15}
V35	NO	PBN 620°C	5×10^{16}
V34	YES	PBN 620°C	1×10^{13}

The reason for the vast difference in the effectiveness of the gallium oxide must be the impurities present in the two starting materials. The extra boron and /or carbon in the LEC M/ACOM must be reducing the effectiveness of the oxide. The reactions occurring, as mentioned in chapter 1, might include the following:

(5) SiO_2 (s) + 2 C (s) = Si (s) + 2 CO (g).

(8) 3 SiO (g) + 2 B (in melt) = B_2O_3 (l) + 3 Si (in melt).

(9) 3 Ga_2O + 2 B (in melt) = B_2O_3 (l) + 6 Ga (in melt).

In the case of the carbon, more appropriate reactions might be:

(10) 2 SiO (g) + C (in melt) = CO_2 (g) + 3 Si (in melt)

(11) Ga_2O (g) + C (in melt) = CO (g) + 2 Ga (in melt)

since there is no solid silica in direct contact with carbon as was the case mentioned in chapter 1. Reactions (8) and (10) show how B and C, if present in significant concentrations, counteract the effect of the oxide on Si. Another effect that boron and carbon in the melt have is that they react with the Ga_2O vapor produced by the oxide addition, as shown in (9) and (11). This in turn, directly reduces the effectiveness of the oxide in preventing silicon contamination.

It should also be noted that when the carrier concentration reaches values as low as 10^{13} cm^{-3}, as in V34, Si may not be the dominant impurity. At the ppb level, other impurities present in the starting material, such as sulfur, selenium, zinc and tin may become important.

3.2.4. Role of the PBN Crucible

Although it has been shown that a PBN crucible increases the silicon contamination in both horizontal gradient freeze[32] and HB[33], when used in conjunction with B_2O_3 encapsulation, the PBN crucible is necessary in order to produce semi-insulating material. This can be seen by comparing the results of V39 and V41. For both, we used the same starting material and growth conditions. The crystal grown in a silica crucible had a carrier concentration of mid 10^{14} cm^{-3} but the crystal grown in PBN was semi-insulating with a concentration of 10^8 cm^{-3} and a resistivity of 2×10^8 $\Omega \cdot cm$.

3.2.5. Effect of B_2O_3 Encapsulation

It has been shown that B_2O_3 with a high water content can be used to suppress Si contamination of the melt for LEC GaAs grown in quartz crucibles[56,57]. Silicon and boron can be incorporated into the melt as discussed in section 3.2.3. Specifically, the reactions are:

(1) 4 Ga (g) + SiO_2 (s) = 2 Ga_2O (v) + Si (in melt).

(9) B_2O_3 (l) + 6 Ga (in melt) = 3 Ga_2O + 2 B (in melt).

However, the presence of moisture in the wet B_2O_3, i. e. the high hydroxyl ([OH]) content, provides an alternative mechanism by which the reaction proceeds by the chemical reduction of water at the expense of the SiO_2 and B_2O_3, thereby inhibiting B and Si contamination from the encapsulant and crucible, respectively.

For V41, we used a dry encapsulant, which has not been shown to inhibit Si and B incorporation. The results of V41 indicate that there is some contamination due to transport from the quartz crucible to the GaAs melt through the thin B_2O_3 coating on the internal surface of the crucible; however, the isolation of the melt from the Si contaminated ambient by the thick B_2O_3 encapsulant (about 5 mm) on top of the melt resulted in a crystal with a carrier concentration that was three orders of magnitude lower than a quartz-crucible-grown crystal with no encapsulant. This can be seen by comparing the average carrier concentrations of V18 and V41, which are 2×10^{17} and 4×10^{14} cm^{-3}, respectively.

It was previously reported that a B_2O_3 encapsulant could purify the melt in a CZ system by gettering silicon[41]. Similarly, it seems that the encapsulant must be gettering silicon in our VGF system since the encapsulant was necessary in order to produce semi-insulating material. Thus, the combination of its ability to purify the melt and its ability to minimize contact between the ambient and the melt are the necessary characteristics which the encapsulant provides so that SI GaAs is achieved.

When the synthesis with the low carrier concentration due to Ga_2O_3 was used for growth with the encapsulant, the material had a low carrier concentration and high resistivity but did not have the usual SI characteristic values. The charge had a carrier concentration of 3×10^{11} cm^{-3}, while that of the crystal V44 was one to two orders of magnitude lower (see Table III). This further supports the conclusion that the encapsulant must be gettering silicon and/or some other impurities that were previously preventing the attainment of high resistivity material.

3.2.6 Role of Carbon

Carbon acts as a shallow acceptor in bulk GaAs. It plays a key role in the compensation mechanism in LEC material, along with EL2, in insuring that the material be semi-insulating. The role of carbon in VGF crystals may be different and needs to be assessed. Thus, the carbon concentration of several crystals was measured by LVM. A spectrum for one of the crystals, V39, is shown in figure 9. The tabulated results are shown in Table VII. It should be noted that the detection limit of the system for carbon in GaAs is approximately 1 x 10^{14} cm^{-3}.

Table VII. Carbon Concentration of Selected Crystals

CRYSTAL	CARBON CONCENTRATION (cm^{-3})
SI M/ACOM charge	1.2 x 10^{15}
V33-1	< 10^{14}
V33-2	< 10^{14}
V34-1	6 x 10^{14}
V34-2	7 x 10^{14}
V39	4 x 10^{15}
Ga_2O_3 Synthesis	< 10^{14}

It can be seen from the data that some of the carbon must be gettered by the encapsulant since the carbon concentration of the starting material (SI M/ACOM) is significantly higher than that of the crystal V33 and there was no oxide to react with the carbon to remove it, as shown above in reactions (10) and (11). V33 was grown with a wet encapsulant, while V39 was grown with a dry B_2O_3 encapsulant. As discussed in 3.2.4, the wet encapsulant has been shown to inhibit the incorporation of boron and silicon for LEC GaAs grown in quartz crucibles, whereas, the dry B_2O_3 was not nearly as efficient [56]. Hunter et. al.[49] have shown that the concentration of carbon in LEC GaAs depends on

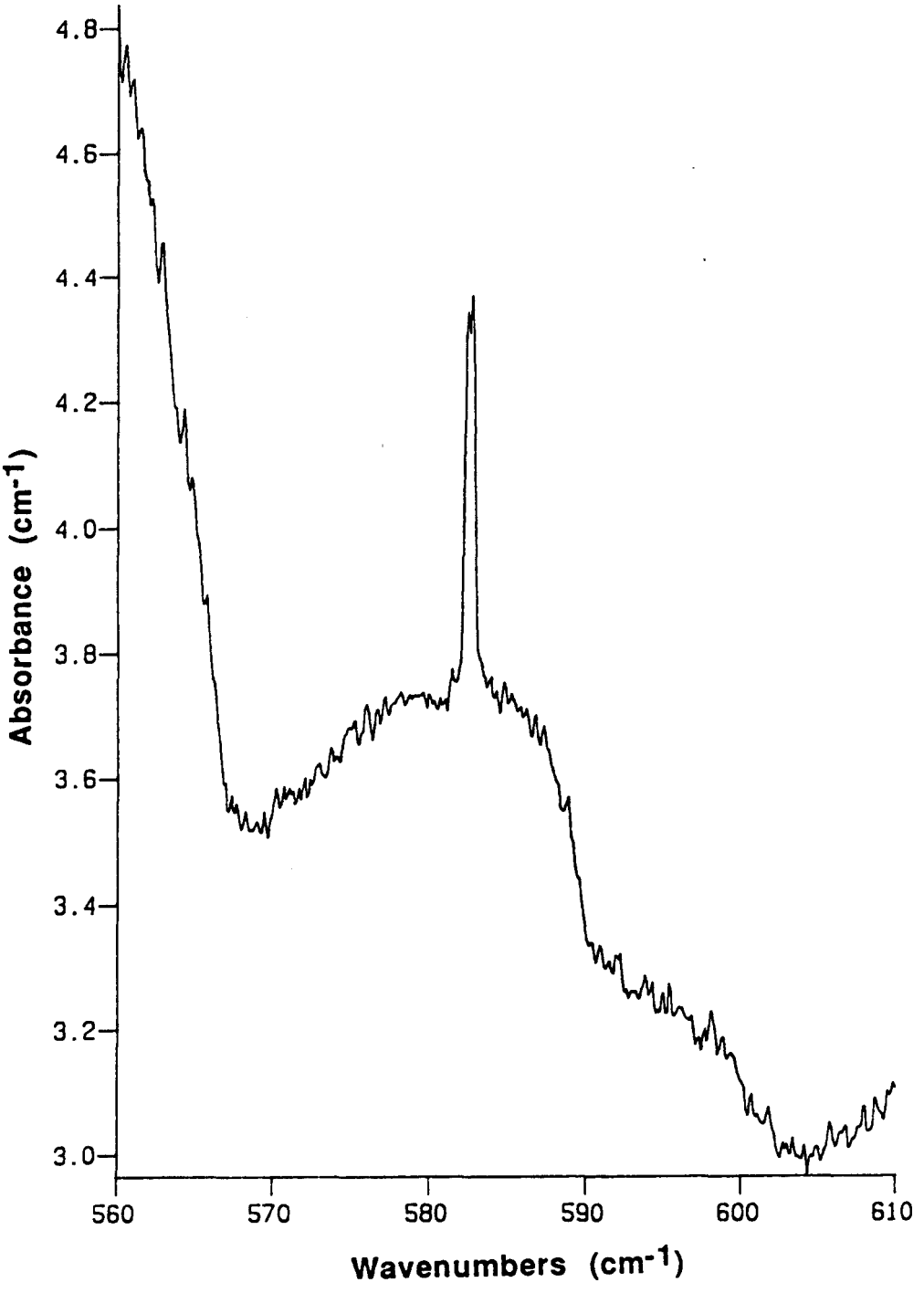

Figure 9. LVM spectrum of V39. Carbon peak observed at 582 cm^{-1}.

the water content of the B_2O_3. They reported the use of dry B_2O_3 (100-150 ppm H_2O) results in carbon concentrations as high as 8 x 10^{15} cm^{-3}, while wet B_2O_3 (500 ppm H_2O) produces concentrations below the detection limit of their system, 3 - 5 x 10^{14} cm^{-3}. V33 and V39 were grown with the same starting material, M/ACOM, which has a high carbon concentration. Our data from these crystals supports the conclusions of Hunter et. al. that the wet encapsulant getters carbon while the dry encapsulant does not. The hydroxyl ions ([OH]'s) apparently react with the carbon in the melt to form CO or CO_2 gas.

V39 and V42, the two semi-insulating crystals, were grown with a dry encapsulant. This fact further substantiates the above statement that a dry encapsulant may not be as effective as a wet encapsulant in gettering or removing carbon (forming CO or CO_2) present in the melt. It also indicates that a dry encapsulant is necessary for the production of SI material with our system. Hunter et. al.[49] concluded that the use of the wet encapsulant for LEC growth leads to too low a carbon concentration which in turn leads to insufficient compensation. Their crystals grown with a wet encapsulant had room temperature carrier concentrations up to 10^{11} cm^{-3}, but those grown with a dry encapsulant produced crystals always below 5 x 10^{7} cm^{-3}.

The relatively high carbon concentration of V39 indicates that carbon is a necessary component in the compensation mechanism of SI GaAs grown in our VGF system. This is further supported by the results of V34 and the Ga_2O_3 synthesis. Neither of these has as much carbon as V39 and neither one is semi-insulating. The average resistivities are 3 x 10^4 and 3 x 10^3 $\Omega \cdot cm$, respectively. The role of carbon in the compensation mechanism of VGF crystals will be studied further. Study is needed because of the presence of the deep levels EL5 and/or EL6. This will be discussed in more detail in section 3.3.

3.2.7 Arsenic Pressure Effects during Growth

It is known that an increased As pressure during growth increases the EL2 concentration in LEC grown crystals. It is also known that EL2 is responsible for the SI behavior of LEC-grown GaAs. Since several of the crystals prior to V40 had low carrier concentrations but were not semi-insulating, it was thought that increasing the arsenic pressure in the growth ampoule in order to increase the EL2 concentration might allow us to obtain SI material. However, increasing the As pressure for V40 did not have the desired effect. It may have increased the EL2 concentration somewhat, but it is clear that it did not increase it enough to produce semi-insulating material. This run was very similar to V34 except for the increased arsenic pressure and the fact that the PBN 620°C charge was Ga-rich. It is unclear what effect the Ga-rich charge has on the growth. However, the crystal has a higher carrier concentration than V34, so the idea was unsuccessful.

3.3 Characterization of the Crystals for Deep Levels

DLTS temperature scans of the early VGF crystals showed EL2 and EL6 to be the dominant deep level defects present in our material. Fig. 10 shows a plot of one of these temperature scans for V18. EL2 is identified at 370K and corresponds to an energy of 0.75eV, while it is known that EL6 occurs around 200K, at an energy of 0.35eV. By obtaining data of the emission rate versus temperature at various time constants, one obtains a plot of emission rate versus inverse temperature. The plot for the peak that was thought to be EL6 is shown in fig.11. The activation energy, obtained from the slope, was found to be 0.345 ± 0.002 eV, which does indeed correspond to the value reported as the deep level EL6. Thus our conjecture was supported.

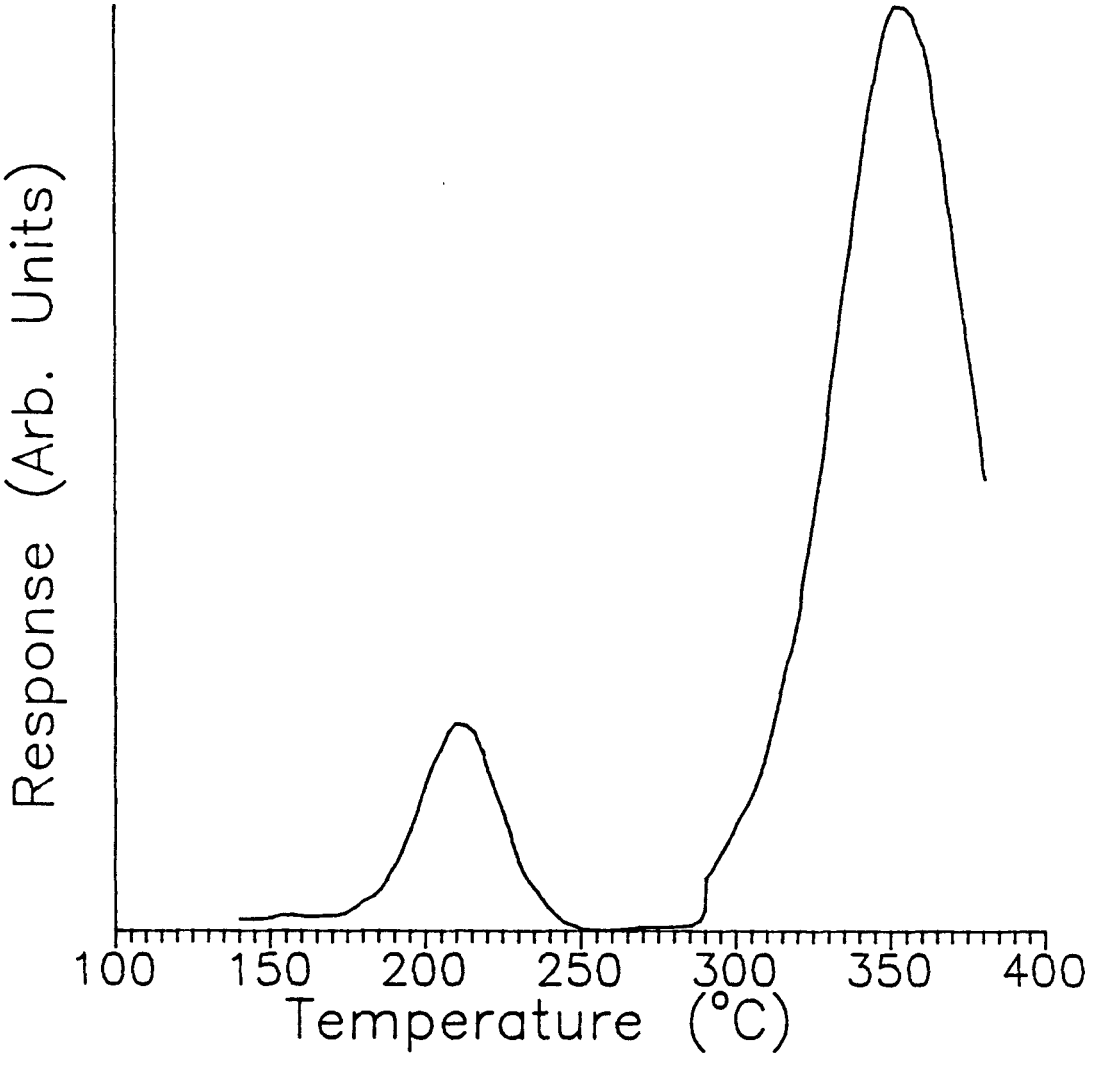

Figure 10. DLTS Response versus temperature for crystal V18.

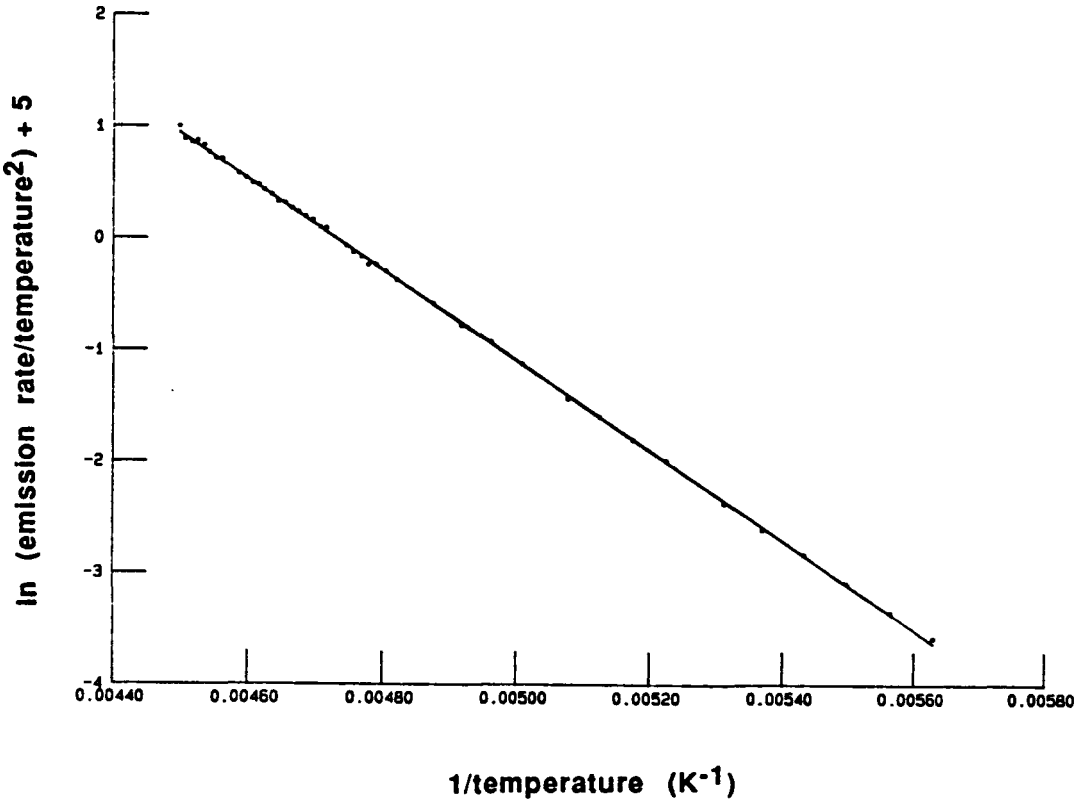

Figure 11. Emission rate versus inverse temperature for V18.

In order for DLTS results to be interpreted in a simple fashion, the concentration of the defect should be less than 10% of the free carrier concentration. For most of the crystals grown in this study, this was not the case since the carrier concentration were quite low. Consequently variable temperature Hall effect had to be used to identify the dominant deep level.

Crystals V33 and V34 are two that have unusually low carrier concentrations, yet they are not semi-insulating. This is quite unusual but has been reported previously by Martin et. al.[58]. The carrier concentration versus fraction solidified for these crystals is shown in figure 12. It can be seen that the values range from 10^{10} to 10^{14} cm^{-3} for each. Variable temperature Hall effect measurements were performed to see if a level might be pinning the Fermi level. The temperatures ranged from 200- 370 K. The carrier concentration as a function of inverse temperature for each crystal is shown in figure 13. The slope of both plots is nearly the same, 0.39 and 0.40 eV, respectively. A Hall-effect level at 0.42 eV is commonly observed in both HB and LEC material[59]. The activation energies reported for EL5 and EL6 are 0.42 and 0.35 eV[60], respectively. Parsey has found EL2, EL5 and EL6 to be the dominant deep level defects in HB-grown GaAs[43]. He reports values of 0.40 and 0.34 eV for EL5 and EL6. Thus it appears that it is either EL5 or EL6 that is pinning the Fermi level in our material. Recently, Look[61] has stated that EL6 (identified by DLTS at an energy of 0.35eV) may be closely related to the 0.42eV Hall-effect center, since their energies are so close and they are the only two centers, other than EL2 commonly seen in the 10^{15} - 10^{16} cm^{-3} range in GaAs. The levels in our crystals will be examined in more detail in the future. It should be noted that these two crystals used different starting materials and different additions in order to reduce the silicon contamination and yet they both have the same deep level in significant concentrations.

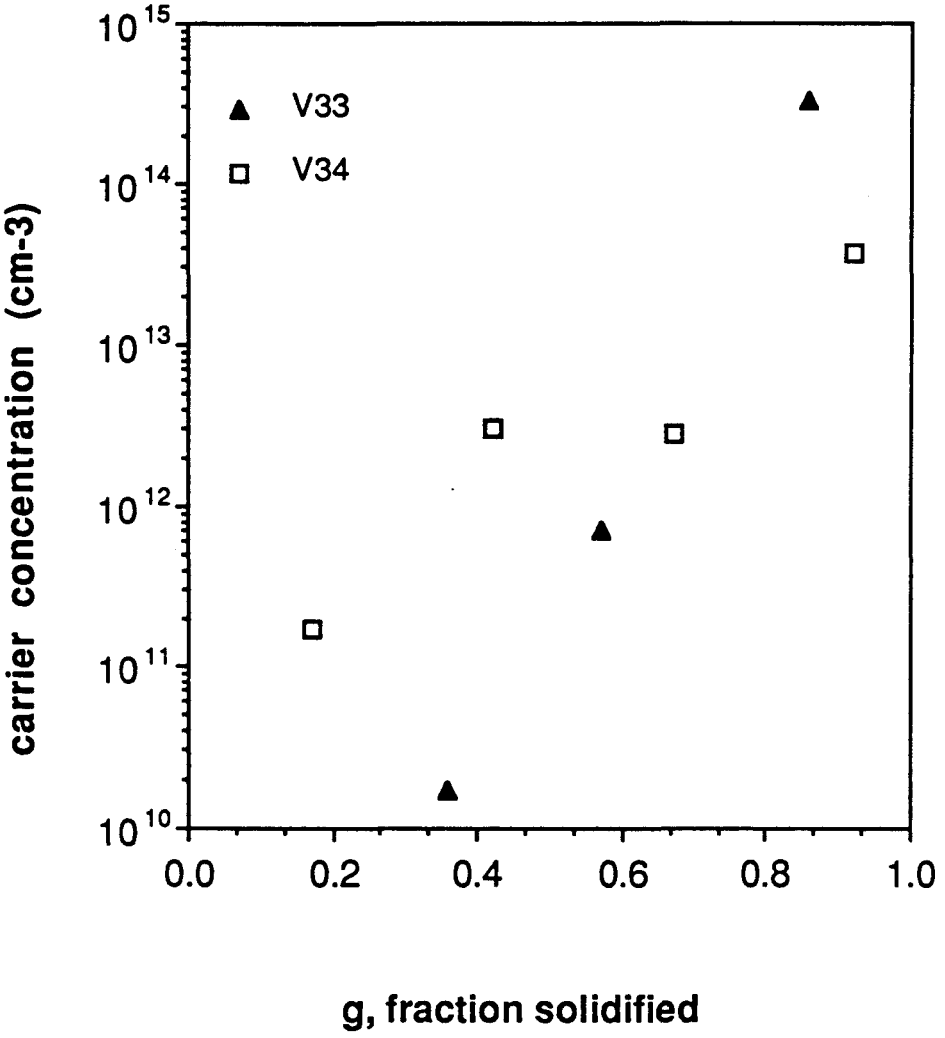

Figure 12. Carrier Concentration versus g, fraction solidified, for crystals V33 and V34.

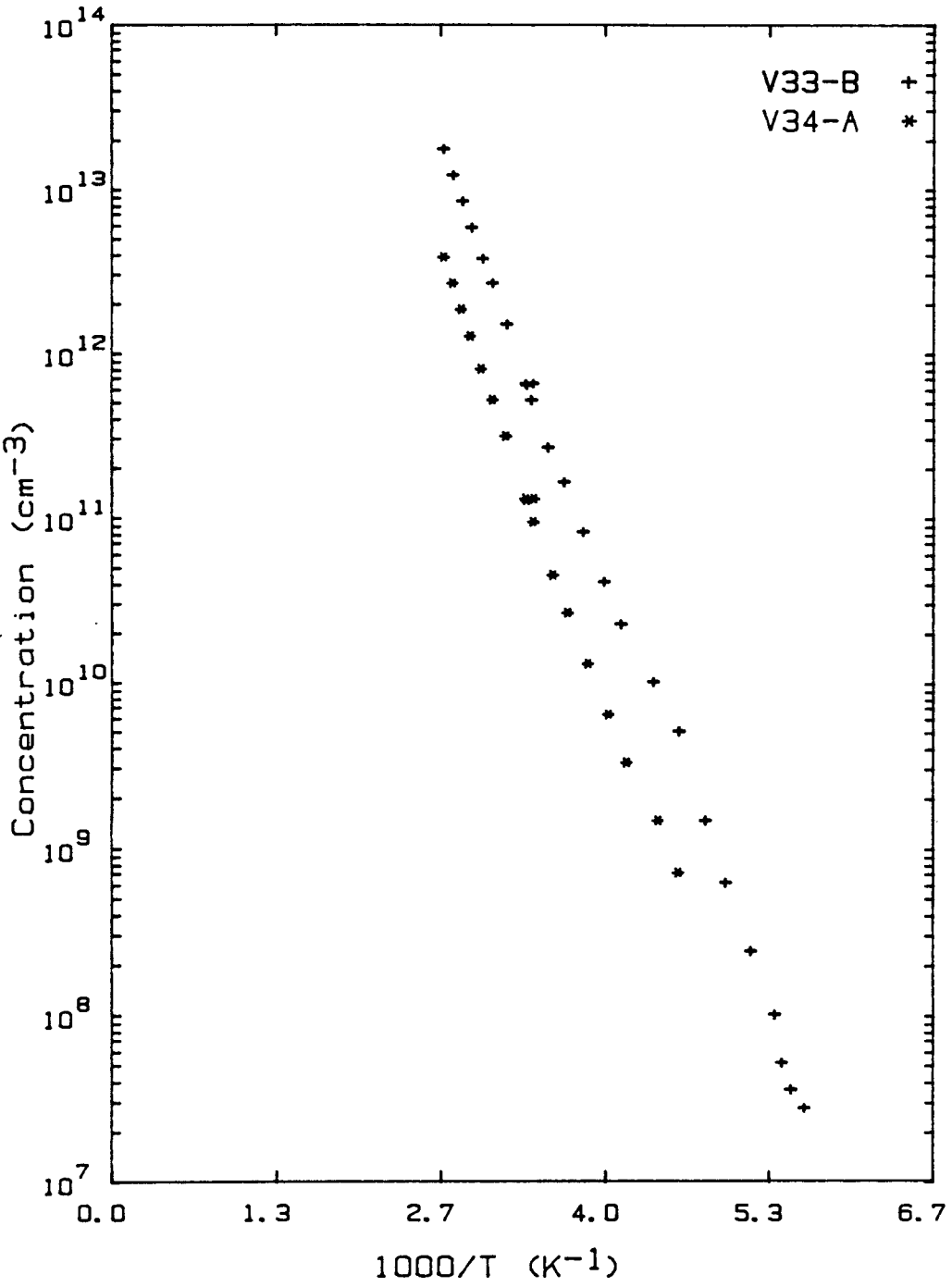

Figure 13. Carrier concentration as a function of inverse temperature for V33 and V34.

LEC material shows an activation energy of 0.75 eV, corresponding to EL2. Abernathy et. al.[23] reported gradient freeze material, both horizontal and vertical, with an activation energy of 0.46-0.54 eV. They concluded that the Fermi level is pinned at a higher level in the gap than EL2, and that consequently, EL2 is not involved in the compensation mechanism in their material. Our results suggest the same conclusion but for a different level.

4. CONCLUSIONS AND FUTURE WORK

The main conclusions that can be drawn from the synthesis experiments are: (1) the silicon contamination does occur via a vapor transport mechanism during synthesis and growth; (2) there is little difference in the carrier concentration when comparing the use of a silica versus a PBN boat for synthesis; (3) gallium oxide can effectively suppress the reduction of SiO_2 and thus limit the amount of Si incorporated into the starting material but there is a limit on the amount of suppression possible during synthesis due to a saturation effect.

Thirteen crystals were grown in this work, two of which were semi-insulating. Three others had fairly high resistivities (10^4 -10^6 Ω-cm) but were not semi-insulating (10^8 Ω-cm). The mobilities were comparable to some reported in the literature. An increase in the mobility should result from the ongoing research to improve the structural perfection of the crystals by eliminating low angle grain boundaries and As precipitates.

Examining the systematic approach to the growth of semi-insulating material with the new vertical gradient freeze system which contains silica, it can be seen that the starting material proved to be a very important factor in the

final product. It is the impurities present in the starting material which are the key to the effectiveness of the silicon contamination control method. The only method of producing SI GaAs appears to be the use of a SI charge in a PBN crucible with total B_2O_3 encapsulation. The encapsulant proved effective since it not only acted as a barrier to convective flow of contaminated gas to the melt, but it also was shown to getter some impurities, specifically carbon and silicon. The hydroxyl content of the encapsulant determines its effectiveness in gettering these impurities.

The capillary tube was shown to be ineffective in our system. This is probably due to the fact that gas flow by convection is dominant over diffusion in our VGF system and since the mechanism by which the tube works involves the control of diffusion, it was ineffective. Both the BN liner tube and the BN cap used for limiting the free volume of space for gases to react in the high temperature end on the furnace, were only slightly effective. The cap serves as a barrier to vapor transport by convection but since it has a hole for stoichiometry control and is not sealed over the crucible, it was not a complete barrier to the flow of contaminated gas to the melt surface. The liner, when combined with the cap, still did not prove to be effective enough in eliminating the flow of contaminated gases to the melt.

Oxygen doping via the addition of Ga_2O_3 to the charge prior to growth did show a significant improvement in producing materials with somewhat high resistivities (10^4-10^6 Ω·cm). The oxide was more effective for our charge than for the LEC charge, probably because the high concentrations of boron and carbon in the LEC material counteracted some of the oxide effect. The B and C may enhance Si contamination and react directly with the Ga_2O produced by the oxide addition, limiting the ability of the oxide to purify the material.

The water content of the liquid encapsulant was another factor found to influence the resulting material. It was previously reported that a wet encapsulant inhibits the incorporation of Si, B and C into the melt. We also found that wet B_2O_3 getters carbon. We speculate that the carbon reacts with the hydroxyls in the wet encapsulant to form CO and CO_2. This is an unfavorable result since it seems that a relatively high carbon concentration is necessary for the production of SI material because of its role in the compensation mechanism. Thus, we suggest that dry B_2O_3 is necessary for the attainment of SI GaAs in our VGF system. However, definite conclusions can not be drawn without further study.

It was determined that a deep donor level, either EL5 or EL6, was pinning the Fermi level and thus preventing the attainment of SI material for the oxygen doped crystals. It is interesting to note that the same level, EL5 or EL6, is present in the first encapsulated crystal, which did not have the oxide addition. This could indicate that oxygen is not responsible for the presence of this level. When the oxide synthesis was used for growth with the encapsulant, the material produced was of high resistivity, however, the Fermi Level was pinned at a level above the mid-gap level EL2.

Further, our results suggest that EL5 and/or EL6, as well as EL2 play a major role in the compensation mechanism in VGF-grown GaAs crystals. An area of future work will be concerned with investigating the above hypothesis.

In the systematic approach to the growth of semi-insulating crystals, a group of crystals which span a wide range of resistivities and carrier concentrations have been produced. These will prove valuable in the future for trying to understand the compensation mechanism involved in VGF-grown GaAs. Techniques such as optical absorption and glow discharge mass spectroscopy (GDMS) will be used to determine the EL2 and silicon

concentrations, respectively . GDMS is a technique that is even more sensitive to impurities in the bulk than SIMS and therefore, has a slightly lower detection limit. It would also be informative to determine the boron concentration of the starting materials, with GDMS or LVM, in order to try to quantify its effect on the resulting crystal. Boron is isoelectronic with Ga but its presence has been shown to affect Si contamination.

Impurity analysis of the starting materials and the resulting crystals, the effect of the water content of the encapsulant and the role of the deep levels and impurities in the compensation mechanism of VGF-grown GaAs are the main areas that need to be researched further. With a reproducible method of growing semi-insulating GaAs that has excellent material uniformity and very low dislocation densities, an understanding of the compensation mechanism and a means of controlling the impurity incorporation during growth, GaAs produced by the new VGF technique will surely play an important role in the future of high performance compound semiconductor devices.

5. REFERENCES

1. G. Muller, Crystal Growth from the Melt, Vol 12 of Crystals: Growth, Properties and Applications, Springer-Verlag Berlin Heidelberg, 1988, p.5.
2. H. Welker, Z. Naturforschg. **7a**, (1952) p. 744, **8a** (1953) p. 248.
3. C. C. Shen and Davis H. Hartman in Gallium Arsenide Technology, David K. Ferry,ed., Howard W. Sams & Co., Inc. (1985) p. 411.
4. H. Unlu and H. Morkoc, Solid State Technology **31** (1988) p.83.
5. David K. Ferry in Gallium Arsenide Technology, David K. Ferry, ed., Howard W. Sams & Co., Inc. (1985) p.5.
6. H. Goronkin, R. O. Grondin and D. K. Ferry in Gallium Arsenide Technology, David K. Ferry, ed., Howard W. Sams & Co., Inc. (1985) p.155.
7. B. Turner, in GaAs Materials Devices and Circuits, edited by M. J. Howes and D. V. Morgan, Wiley, New York, 1985, p.361.
8. C. W. Tu, R. H. Hendel, and R. Dingle, in Gallium Arsenide Technology, ed. by D. K. Ferry, Howard W. Sams & Co., Inc. (1985) p.107.
9. M. T. Yuan, W. V. McLevige, and H. D. Shih, in VLSI Electronics, Vol. 11, ed. by N. G. Einspruch and W. R. Wisseman, Academic Press, New York, 1985, p.173.
10. C. G. Kirkpatrick, R.T.Chen, D. E. Holmes, P. M. Asbeck, K. R. Elliot, R. D. Fairman, and J. R. Oliver, in Semiconductors and Semimetals, Vol. 20, R. K. Willardson and Albert C. Beer, eds., Academic Press, Inc., 1984, p.161.
11. D. E. Holmes, R. T. Chen, K. R. Elliot, and C.G. Kirkpatrick, Appl. Phys. Lett. **40** (1982) p.46.
12. J. Blanc and L. R. Weisburg, Nature **192** (Oct. 14, 1961) p.155.
13. Swiggard, S. H. Lee, and F. W. Von Batchelder, Conf. Ser.-Inst. Phys. **45** (1979) p. 125.

14. J. Czochralski, Z. Physik Chem. **92** (1918) p.219.

15. R. Gremmelmaier, Z. Naturforsch **11a** (1956) p.511.

16. E. P. A. Metz, R.C. Miller, and R. Mazelsky, J. Appl. Phys. **33** (1962) p.2016.

17. J. B. Mullin, B. W. Straughan, and W.S. Brickell, J. Phys. Chem. Solids **26**, (1965) p.782.

18. P. W. Bridgman, Proc. Amer. Acad Arts Science **60** (1925) p.305.

19. D. C. Stockbarger, Review of Scientific Instruments **7** (1936) p.133.

20. F. Stober, Z. Krist. **61** (1925) p.299.

21. J. M. Parsey and F.A. Thiel, J. Crystal Growth, **73** (1985) p.211.

22. Edith D. Bourret, J. B. Guitron, and E. E. Haller, J. Crystal Growth **85** (1987) p.211.

23. E. M. Monberg, H. Brown and C. E. Bonner, J. Crystal Growth **94**, (1989) p.109.

24. A. S. Jordan and J. M. Parsey, "Growth and Characterization of GaAs Single Crystals," in MRS Bulletin, October 1988, p.36.

25. E. D. Bourret, J. B. Guitron, M. L. Galiano, and E. E. Haller, to be presented at The Ninth International Conference on Crystal Growth, Sendai, Japan, Aug. 20-25, 1989.

26. Chong E. Chang, Vincent F. S. Yip and William R. Wilcox, J. Crystal Growth **22** (1974) p.247.

27. W. A. Gault, E. M. Monberg and J. E. Clemans, J. Crystal Growth **74**, (1986) p.491.

28. J. Conway and J. E. Clemans, Proceedings of the 5th Conference on Semi-insulating III-V Materials, (Malmo, Sweden, June 1-3,1988) ed. by G. Grossmann and L. Lebedo, p.423.

29. C. R. Abernathy, A. P. Kinsella, A. S. Jordan, R. Caruso, S. J. Pearton, H. Temkin, and H. Wade, J. Crystal Growth **85** (1987) p.106.

30. C. N. Cochran and L. M. Foster, J. Electrochem. Soc. **109**, (1962) 149.

31. J. R. Knight, Nature **185** (1961) p.1001.

32. Robert I. Stearns and James B. McNeely, J. Appl. Phys. 37 (1966) p.933.

33. T. Kobayashi, J. Lagowski, and H. C. Gatos, Proceedings of the 5th Conference on Semi-insulating Materials III-V Materials, (Malmo, Sweden, June 1-3,1988) ed. by G. Grossman and L. Ledebo.

34. C. N. Cochran and L. M. Foster, J. Electrochem. Soc. **109**, (1962) p.144.

35. Eishi Kubota and Akinori Katsui, J. Crystal Growth **82** (1987) p.573.

36. Takasi Shimoda and Shin-ichi Akai, J. J. Appl. Phys. **8** (1969) p.1352.

37. N. G. Ainslie, S. E. Blum, and J. F. Woods, J. Appl Phys. **33** (1962) p.2391.

38. J. F. Woods and N. G. Ainslie, J. Appl. Phys. **33** (1963) p.1469.

39. S. E. Blum and R. J. Chicotka, J. Electrochem. Soc. **120** (1973) p.588

40. A. Goetzberger and W. Schockley, J. Appl. Phys. **31** (1960) p.1821.

41. Kazutaka Terashima, Hiroaki Nakajima and Tsuguo Fukuda, J. J. Appl. Phys. **21**, (1982) p. L452.

42 R. H. Mellen, Sr., US Patent Nos. 4,086,424, 4,423,516 and 4,518,351.

43. J. M. Parsey, Ph. D. Thesis, MIT, 1983.

44. T. S. Plaskett, J. M. Woodall, and A. Segmuller, J. Electrochem. Soc., **118** (1971) p.115.

45. J. M. Parsey, Y. Nanishi, J. Lagowski, and H. C. Gatos, J. Electrochem. Soc. **129** (1982) p.388.

46. M. S. S. Yong, R. Caruso, J. M. Parsey, and A. P. Kinsella, unpublished work, referenced in Abernathy, et. al. (ref. 23).

47. L. J. van der Pauw, Phillips Res. Repts. **13** (1958) p.1.

48. G. A. Gledhill, R. C. Newmann and J. D. Collins, Proceedings of the 6th International Conference of Fourier Transform Spectroscopy, Vienna, 1987.

49. A. T. Hunter, H. Kimura, J. P. Baukus, H. V. Winston, and O. J. Marsh, Appl. Phys. Lett. **44** (1984) p.74.

50. M. R. Brozel, E. J. Foulkes, R. W. Series and D. J. T. Hurle, Appl. Phys. Lett. **49** (1986) p.337.

51. W. M. Theis, K. K. Bajaj, C. W. Litton and W. G. Spitzer, Appl. Phys. Lett. **41** (1982) p.70.

52. R. J. Blattner and C. A. Evans, Jr., "High-Performance Secondary Ion Mass Spectrometry," Scanning Electron Microscopy/1980/IV SEM Inc., AMF O'Hare (Chicago), IL.

53. D. V. Lang, J. Appl. Phys. **45** (1974) p.3023.

54. J. L. Hurd, D. L. Perry, B. T. Lee, K. M. Yu, E. D. Bourret, and E. E. Haller, to be published in J. Materials Research, 1989.

55. M. L. Gray, J. E. Clemans, and K. A. Grim, in Defect Recognition and Image Processing in III-V Compounds II, ed. by E. R. Weber, Elsevier Scientific Publishers B. V., Amsterdam, 1987, p.25.

56. R. D. Fairman, R. T. Chen, J. R. Oliver and D. R. Chen, IEEE Trans. Electron Devices **ED-28** (1981) p.135.

57. J. R. Oliver, R. D. Fairman, R. T. Chen and P. W. Yu, Electron. Lett **17** (1981) p.839.

58. G. M. Martin, J. P. Farges, G. Jacob,, and J. P. Hallais, G. Poiblaud, J. Appl. Phys. **51** (1980) p. 2840.

59. D. C. Look, S. Chaudhuri, and J. R. Sizelove, Appl. Phys. Lett. **42** (1983) p.829.

60. G. M. Martin, A. Mittonneau, and A. Mircea, Electronic Letters **13** (1977) p. 191.

61. David C. Look, Proceedings of the 5th Conference on Semi-insulating III-V Materials, (Malmo, Sweden, June 1-3,1988) ed. by G. Grossmann and L. Lebedo, p. 1.